

The Temperature-Dependent Deformation of Nafion for Fuel Cell Applications

Alison Brittany Lehr
May 16th, 2005
Professor Jay Benziger

Submitted in partial fulfillment
of the requirements for the degree of
Bachelor of Science in Engineering

Department of Chemical Engineering and
Materials Science and Engineering Certificate Program

Princeton University

I hereby declare that I am the sole author of this thesis.

I authorize Princeton University to lend this thesis to other institutions or individuals for the purpose of scholarly research.

Alison Lehr

I further authorize Princeton University to reproduce this thesis by photocopying or by other means, in total or in part, at the request of other institutions or individuals for the purpose of scholarly research.

Alison Lehr

Princeton University requires the signatures of all persons using or photocopying this thesis.
Please sign below and give address and date.

To my family, friends, peers,
and all those that make my life enjoyable.

Acknowledgements

First and foremost I'd like to thank my parents and the rest of my family for their support and encouragement. I'd like to thank Professor Benziger for allowing me to work with him, coming up with a thesis topic that would be the most interesting to me, and guiding me along the way. I also appreciate the assistance and advice offered by Barclay, James, and Warren that helped me get all the way through my lab work.

I am very grateful to Professor Arnold for providing me with countless ideas to get passed obstacles and lending me materials to get started. I am greatly indebted to Helena Gleskova, Joe Palmer, and all the graduate students that took time out of their schedules to help me along in the clean room. This thesis would not have been successful without the help of Jane Woodruff, who took significant time out of her day to assist me with the Scanning Electron Microscope.

And last, but not least, I'd like to thank all my classmates for reminding me that, even in the worst of times, my favorite part of this major is the camaraderie among the students.

Abstract

Fuel cells are a clean and efficient means of producing electricity. Polymer Electrolyte Membrane Fuel Cells (PEMFCs) commonly use Nafion, a polymer electrolyte, to conduct protons from the anode to the cathode. Since protons are conducted by means of the hydronium ion (H_3O^+), the membrane must be humidified to function. Operation of a PEMFC at variable water activity has suggested that the polymer membrane swells as it absorbs water[1]. Because the polymer membrane is constrained between porous electrodes, it will expand into the pores as it swells and likely contact a greater surface area of catalyst, thereby improving fuel cell performance. To mimic the deformation of Nafion into an electrode, a piece of Nafion was pressed on top of a silicon wafer etched with trenches of various widths and the cross section was viewed in the SEM. It was found that the deformation of Nafion was very dependent on the temperature at which it was pressed. If pressed above or close to its glass transition temperature, Nafion completely deformed into features with widths of 5 μm and greater. At no temperature did the Nafion fully deform into a 2 μm feature, suggesting 2 μm was a critical pore size. The manner in which the Nafion deformed has important implications for fuel cell operation, MEA fabrication, electrode morphology, and membrane thickness.

Table of Contents

<i>Acknowledgements</i>	<i>v</i>
<i>Abstract</i>	<i>vi</i>
<i>Table of Contents</i>	<i>vii</i>
<i>Table of Figures</i>	<i>ix</i>
<i>1. Introduction</i>	<i>1</i>
1.1 Motivation	1
1.2 Goals	3
<i>2. Fuel Cells</i>	<i>4</i>
2.1 How Fuel Cells Work	4
2.2 Why Polymer Electrolyte Membrane Fuel Cells (PEMFCs)	5
2.3 Limits of PEMFCs	5
<i>3. Nafion</i>	<i>7</i>
3.1 As a Copolymer	7
3.2 As an Ionomer	7
3.3 Structure of Nafion	8
3.4 Properties of Nafion	10
3.4.1 Equivalent Weight	10
3.4.2 Glass Transition	11
3.4.3 Mechanical Properties	12
<i>4. Membrane-Electrode Assembly (MEA)</i>	<i>14</i>
4.1 Structure of the Electrode	14
4.2 Procedure	15
<i>5. Experimental Procedure</i>	<i>17</i>
5.1 Creation of the Mask	17
5.2 Photolithography	19
5.3 Reactive Ion Etching (RIE)	20
5.4 Hot Pressing	21
5.4.1 Temperature Selection	22
5.5 Difficulties in Sample Preparation	24
5.5.1 Wet Samples	24
5.5.2 Fracturing in Liquid Nitrogen	25
<i>6. Results and Discussion</i>	<i>26</i>
6.1 The Effect of Temperature	27
6.1.1 At 140 degrees Celsius	27
6.1.2 At 60 degrees Celsius	28

6.2 Behavior Around the Glass Transition Temperature	30
6.2.1 Stress features	32
6.3 Nafion Deformation in 2 micron Features	34
7. Conclusions	39
7.1 Importance for Fuel Cell Operation	39
7.2 Importance for MEAs	40
7.3 Importance for Electrode Morphology	41
7.4 Importance for Membrane Thickness	42
7.5 Recommendations for further study	42
References	45
Appendices	A-1
Photolithography Recipe	A-2
Additional SEM Pictures at 90 °C	A-3
Additional SEM Images at 100 °C	A-6
Additional SEM Pictures at 110 °C	A-8
Additional SEM Pictures at 140 °C	A-10

Table of Figures

Figure 1 Schematic of a simple fuel cell	1
Figure 2 (Left) Dynamic response of the STR PEM fuel cell for switching the load resistance from 20 to 7 Ω at 80°C [3]. (Right) The Nafion membrane pressing in between the catalyst-coated carbon particles in the electrode	2
Figure 3 Schematic of a fuel cell [4].	4
Figure 4 CO coverage on a platinum surface as a function of temperature and CO concentration. H_2 partial pressure is 0.5 bar[5].	6
Figure 5 Chemical structure of Nafion in its acid form where $m = 1, 2$, or 3 ; n typically has a value in the range of 6-7, and ∞ is about 1000 [8]	7
Figure 6 Schematic representation of redistribution of ion exchange sites which occurs on dehydration of the polymer [12].	9
Figure 7 Three regions structural model for Nafion [13].	10
Table 1 Glass Transition temperature (in °C) of Nafion in its acid form as determined by different techniques	11
Figure 8 10-sec modulus vs. temperature for Nafion-H, Nafion-K, PS, PS 3.8 (Na)h, and PS 7.9 (Na)1. Curves for styrene and two styrene ionomers are shown for comparison[11].	12
Table 2 Physical properties of Nafion membranes. MD stands for machined direction, TD for transverse direction, and RH for relative humidity [14]	13
Figure 9 Schematic of the cross-section of a fuel cell consisting of the gas-diffusion electrodes, catalyst layers, and the polymer electrolyte membrane. The gas-diffusion backing fibers are coated with PTFE so as to be not flooded with water, while the catalyst layers comprise ionomer solution among Pt/ C particles for proton transport[15].	14
Table 3 Descriptions of the thirteen different line combinations that appear on the mask to be transferred to the silicon wafer.	18
Figure 10a Schematic showing layer of photoresist on top of Silicon wafer	20
Figure 10b Schematic showing patterning in photoresist after developing. The developer washes away the photoresist exposed to UV light, revealing the silicon wafer beneath.	20
Figure 11a Schematic of photoresist and silicon wafer after RIE. The photoresist acts as a mask so only the exposed areas of the silicon are etched.	21
Figure 11b Schematic of the final etched silicon wafer after the photoresist is removed.	21
Figure 12 Diagram showing sequence of materials pressed on top of each other. The lines etched in the Si wafer are designed to mimic the spacing in the electrode pressed on the top side of the Nafion.	22
Table 4 Conditions under which each sample was etched and pressed. All samples were pressed at a force of 2,000 lb _f and a time of 90 seconds.	23
Image 1 Overview of how Nafion-silicon complex appears in the SEM. The Nafion is on the top, the etched silicon wafer is on the bottom	26
Image 2 - SEM image of sample 4 (140°C). Nafion completely pressed into the 5 μ m feature. Nafion on bottom, silicon wafer on top.	27
Image 3 SEM image of sample 15 (140C). Nafion did not press all the way into the 2 μ m feature. Nafion is on the bottom, silicon is on the top.	28
Image 4 SEM image of sample 20 (60C). Nafion exhibited no deformation.	29
Image 5 SEM image of sample 27 (90C). Nafion deformation into 2 micron features. Nafion on top with pieces of the trench walls stuck in the Nafion.	30

Image 6 SEM image of sample 27 (90C). The Nafion did not completely press into the 15 micron feature. Nafion is on the top, silicon is on the bottom.	31
Image 7 SEM image of sample 17 (100C). Glassy behavior evident in the Nafion. Only Nafion is shown.	33
Image 8 SEM Image of sample 4 (140C): the reverse curvature of Nafion in a 2 micron feature. Nafion is on the bottom, silicon is on the top.	35
Figure 13 Einstein's equation relating the diffusion coefficient D to the Brownian displacement x and time t	36
Figure 14 WLF equation depicting effect of temperature on zero-shear viscosity	37
Figure 15 A plot of Temperature vs. viscosity ratio using the WLF equation.	38
Figure 16 (Left) Cross section of Nafion pressed onto a silicon wafer. (Right) Cross section of Nafion pressed onto an electrode.	39
Figure 17 Nafion contacting carbon particles in electrode at high water content (Left) and low water content (Right)	40
Image 9 SEM Image of 5 micron trench separated by 2 microns pressed at 90C (sample 27).	A-3
Image 10 SEM Image of 10 micron wide trench separated by 2 microns pressed at 90C (sample 27).	A-4
Image 11 SEM Image of a 15 micron wide trench separated by 2 microns pressed at 90C (sample 27)	A-5
Image 12 SEM Image of 2 micron wide features separated by 2 microns at 100C (sample 17)	A-6
Image 13 SEM Image of 5 micron features raised in Nafion separated by 5 microns pressed at 100C (sample 17)	A-7
Image 14 SEM Image of silicon (top) pulled away from Nafion (bottom) pressed at 110C (sample 34)	A-8
Image 15 SEM Image of 2 micron features separated by 2 microns pressed at 110C (sample 34)	A-9
Image 16 SEM image of 2 micron wide trenches separated by 5 microns pressed at 140C (sample 4)	A-10
Image 17 SEM image of 2 micron wide trenches separated by 10 microns pressed at 140C (sample 4)	A-11
Image 18 SEM image of 2 micron wide trench pressed at 140C (sample 4)	A-12
Image 19 SEM image of 2 micron wide trenches pressed at 140C (sample 15)	A-13
Image 20 SEM image of 2 micron wide trenches pressed at 140C (sample 15)	A-14
Image 21 SEM image of 2 micron wide trenches pressed at 140C (sample 15)	A-15
Image 22 SEM image of 10 micron wide trenches separated by 5 microns pressed at 140C (sample 4)	A-16

1. Introduction

1.1 Motivation

Since the late 1980s, strict emissions standards on environmental pollutants and international concern about climate change due to carbon dioxide have inspired the government and academia to research cleaner energy alternatives. Fuel cells are an attractive alternative because of their high efficiency and low pollution.

A fuel cell is an electrochemical device similar to a battery, but designed for continuous replenishment of reactants rather than being limited to an internal storage capacity. Hydrogen fuel is oxidized at the anode and oxygen in the air is reduced at the cathode. The anode and cathode must be physically separated to keep the reactants from mixing. A chemical conduction bridge (such as a membrane) permits the protons to pass from the anode to the cathode. The electrons pass through an external circuit and can be used for electricity. A simple fuel cell is shown in Figure 1.

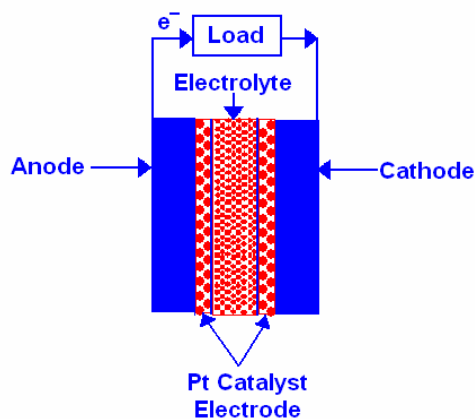


Figure 1 Schematic of a simple fuel cell

There are five classes of electrolytes that can function in fuel cells, and thus there are five types of fuel cells. Polymer electrolyte membrane fuel cells (PEMFCs) are commonly used because of their high power density, specific power, energy efficiency, low operating temperature, and short start-up times (compared to other fuel cell types)[2]. They employ a

functionalized polymer to conduct protons from the anode to the cathode. The interface being investigated in this thesis is that between the electrolyte and the platinum (Pt) catalyst electrode, shown on the right in Figure 2.

Recently, in a paper by Benziger et al.[3], a PEMFC was modeled as two coupled stirred tank reactors (STRs). This arrangement allowed the system response to be analyzed as a function of parameters that could be controlled. One of the phenomena observed was the cell's dynamic response to changes in load. After decreasing the load from 20 to 7 Ω , the response of the cell was measured by plotting cell current and relative humidity vs. time. The result is shown below in Figure 2.

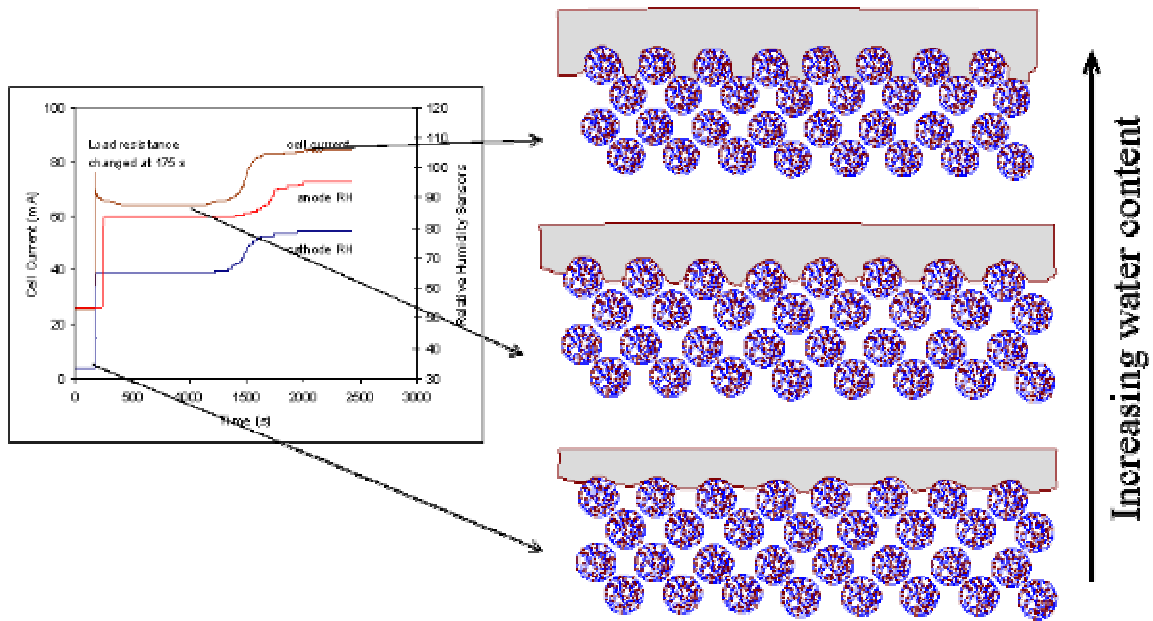


Figure 2 (Left) Dynamic response of the STR PEM fuel cell for switching the load resistance from 20 to 7 Ω at 80°C [3]. (Right) The Nafion membrane pressing in between the catalyst-coated carbon particles in the electrode.

The increase in the fuel cell's current after 1500 seconds was not predicted and occurred even though no variables were changed. Benziger et al. attribute the jump in current to the swelling of the Nafion membrane.

Changing the load affects the amount of water produced. An increase in water production causes the Nafion to swell in a confined area, thereby putting stress on the membrane. It is believed that when the Nafion swells it presses into the neighboring electrode to the extent that it contacts another layer of catalyst particles, which it did not previously reach. The large, circular particles in Figure 2 are carbon particles about 1 μm in diameter with a very high surface area. The carbon particles are sputter-coated with Pt, which is required to oxidize the hydrogen. It is very important that a three phase interface exist in which the Pt, hydrogen, and Nafion all contact each other. If the Nafion indeed does contact a second layer of molecules, more protons will be transported through the membrane and the overall performance of the fuel cell will improve. To investigate this theory, it is important to understand how Nafion conforms to a porous electrode surface.

1.2 Goals

This thesis examines the deformation of Nafion, a polymer electrolyte, into a silicon wafer designed to model an electrode surface. The structure of the membrane-electrode interface and its preparation for use in a fuel cell is discussed in greater detail in section 4. To mimic the pressing of the Nafion into the electrode, a piece of Nafion was pressed on top of a silicon wafer, which was etched with trenches of widths ranging from 2 to 50 microns and average depths of 5 microns. After pressing, the Nafion-silicon laminate was freeze fractured and the cross section was examined in a Scanning Electron Microscope (SEM). The temperature of the pressed samples was varied to observe its effect on the deformation of Nafion.

2. Fuel Cells

2.1 How Fuel Cells Work

Fuel cells are a class of devices that directly convert chemical energy to electricity. A schematic of a fuel cell is shown in Figure 3.

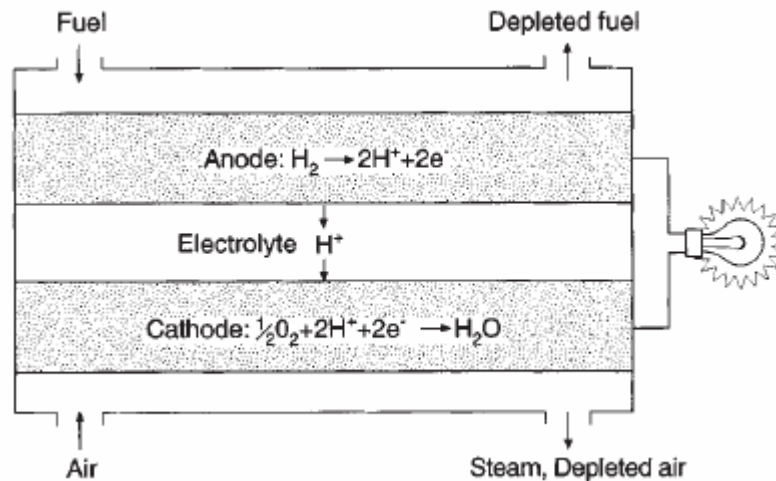


Figure 3 Schematic of a fuel cell [4].

It is composed of three main parts: an anode, cathode, and electrolyte. Hydrogen fuel is oxidized at the anode to create hydrogen ions, or protons, and free electrons. The electrolyte is an electrical insulator, so the electrons must travel through an external circuit to reach the cathode. The protons pass through the electrolyte to the cathode where they combine with oxygen and the free electrons to form water.

To function in a fuel cell, the electrolyte must be able to withstand the operating conditions. It must be chemically stable in hydrogen and oxygen and have an ionic conductivity of at least 0.1 S/cm[4]. Due to these limitations, there are only five classes of materials that can serve as electrolytes: potassium hydroxide, phosphoric acid, perfluorinated sulfonic acid resins, molten carbonate salts, and oxide-ion-conducting ceramics. Here we consider PEMFCs, which employ a perfluorosulfonic acid membrane.

2.2 Why Polymer Electrolyte Membrane Fuel Cells (PEMFCs)

The transportation sector is often cited as a large producer of greenhouse gases and other air pollutants. To decrease emissions, car companies are exploring power sources such as fuel cells for electric vehicles. Polymer electrolyte membrane fuel cells (PEMFCs) are an excellent choice because of their ability to attain a high specific power, power density, and energy density[2]. Their low operating temperature and short start-up times (compared to other fuel cells) are also particularly attractive to the transportation industry.

2.3 Limits of PEMFCs

While PEMFCs have many advantages, they also have some disadvantages. The Pt/C electrode is very sensitive to the presence of carbon monoxide (CO). CO adsorbs to the surface of the electrocatalyst, thereby blocking sites for H₂ adsorption. It is only tolerated in very small amounts; for example, at normal operating conditions 10 ppm is considered the maximum impurity level before CO poisons the catalyst[2].

Protons are transported through the Nafion membrane by means of the hydronium ion (H₃O⁺). Thus, the membrane must be humidified for the fuel cell to function. If the membrane is not properly humidified it does not conduct protons, halting the production of electrical current and water. This requirement imposes an upper limit for the temperature at which the fuel cell can operate. PEMFCs typically operate between 50 and 90°C [2]. Unless the cell operates at a pressure greater than 1 atm, humidification can not be maintained at temperatures greater than 100°C.

Current research is exploring materials to allow PEMFCs to operate at higher temperatures. As temperature increases, reaction and diffusion rates also increase. Furthermore, at higher temperatures, the tolerance of CO in the fuel cell increases. Figure 4

shows the equilibrium coverage of CO at three different concentrations and temperatures ranging from 50-250°C.

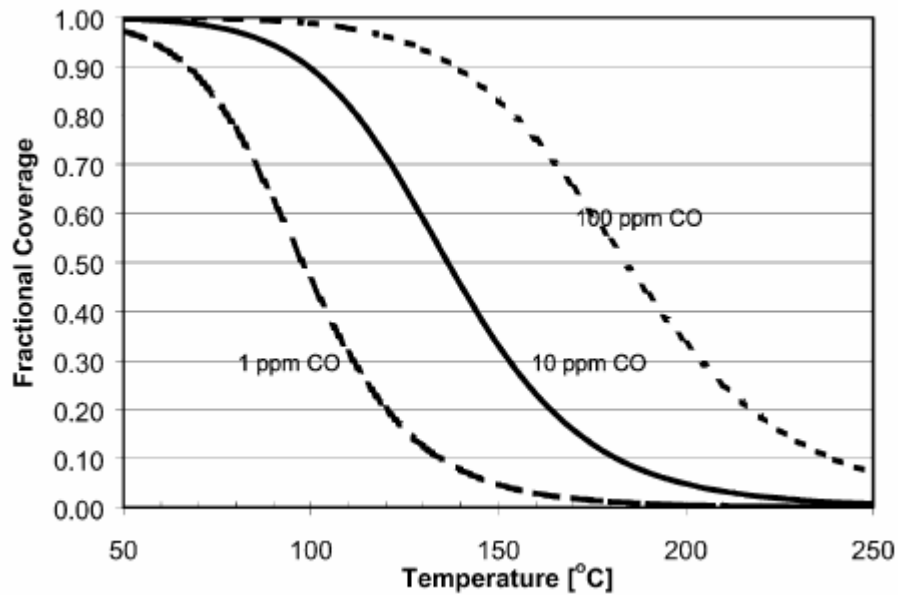


Figure 4 CO coverage on a platinum surface as a function of temperature and CO concentration. H_2 partial pressure is 0.5 bar[5].

Figure 4 shows that for a 10 ppm concentration of CO, the fractional coverage is 90% at 100°C but decreases to 10% at about 180°C. Similar trends follow for the other concentrations – less CO is adsorbed at higher temperatures. In addition to a higher tolerance for CO, at elevated temperatures less water will be present in areas surrounding the membrane. This decrease in water will increase the exposed surface area of the catalyst and enhance the ability of the reactants to diffuse[6].

3. Nafion

3.1 As a Copolymer

NASA first used Nafion in a fuel cell in 1966. Three years later in 1969, Nafion was available for commercial use as a membrane in PEMFCs[7]. Nafion is a copolymer synthesized from tetrafluoroethylene (TFE) and perfluorosulfonylfluoride ethyl propyl vinyl ether (PSEPVE) monomers. Its structure is shown in Figure 5.

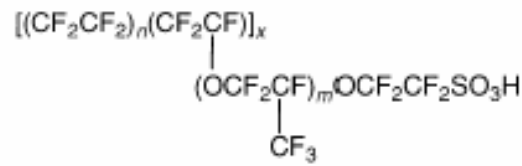


Figure 5 Chemical structure of Nafion in its acid form where m = 1, 2, or 3; n typically has a value in the range of 6-7, and x is about 1000 [8]

Polytetrafluoroethylene (PTFE), more commonly known by its trade name Teflon, is hydrophobic and forms the backbone of the polymer (the CF₂ repeating groups at the top of Figure 5). PSEPVE is a vinyl ether that is useful as a comonomer because it can introduce a side chain functionality that can be converted to sulfonic acid groups[9]. These sulfonic acid groups, shown as the SO₃H at the right of Figure 5, are hydrophilic.

3.2 As an Ionomer

By definition, Nafion is an ionomer, which is a polymer composed of macromolecules in which a small but significant portion of the constitutional units have ionizable or ionic groups, or both[10]. Ionic groups can greatly affect the properties of a given material, in large part because internal ionic attractions change the structure of the material. Polymer electrolyte membranes are based on ionomers where the anion is covalently linked to the polymer backbone and the cation has been ion exchanged with protons. The most widely used PEM is Nafion, a perfluorosulfonic acid manufactured by

DuPont. Other ionomers that have been employed in fuel cells include polystyrene sulfonate (PSS), sulfonated polybenzimidazole (PBI), sulfonated polyether ether ketone (PEEK), etc. These polymers are phase separated with hydrophobic regions and acidic hydrophilic regions. Acid moieties in the hydrophilic regions are ionized when the polymers absorb water. The ionized protons conduct a proton current. Water absorption swells the hydrophilic regions, improving proton conductivity.

3.3 Structure of Nafion

A description of the supermolecular level structure of Nafion was first proposed by Yeo and Eisenberg[11] in 1977. They used small-angle x-ray scattering (SAXS) and dynamic mechanical analysis (DMA) to determine that the ions in the material are clustered, i.e., present in large aggregates also containing some fluorocarbon material. Nafion closely resembled other organic ionomers analyzed in the study, except in the dramatic decrease in density upon ionization accompanied by an increase in the diffusion coefficient for water.

A more precise prediction of the molecular structure of Nafion was offered by Gierke et al[12] in 1981 after performing a detailed study of the ionic clustering in Nafion. Gierke predicted the ionic regions to be spherical with interconnecting channels. He used SAXS and wide-angle x-ray diffraction (WAXD) to analyze both the hydrated and dehydrated forms of Nafion and found excellent agreement with his prediction.

The perfluorosulfonic acid exchange site is a very strong acid and is completely dissociated in water. Thus, a remarkably high degree of water uptake was observed in the perfluorinated ionomer, as much as 50% by volume for 944 equivalent wt. polymer[12]. The water absorption promoted the ionic clustering. SAXS scans of hydrated Nafion confirmed

that the relative electron density of the clusters increased with decreasing water content, implying that the water aggregated in the ion clusters.

By process of elimination, Gierke asserted the model of clustering present was an approximately spherical, inverted micellar structure. This structure satisfied the strong tendency for the sulfonic acid sites to be hydrated and minimized the unfavorable interactions between water and the fluorocarbon matrix. Ionic clustering also existed in the dry polymer. As the polymer absorbed more water, the cluster diameter, exchange sites per cluster, and water molecules per exchange site all increased.

Growth of clusters appeared to occur by a combination of expansion and a continuous reorganization of exchange sites so there were actually fewer clusters in the fully hydrated sample. This reorganization is shown in Figure 6.

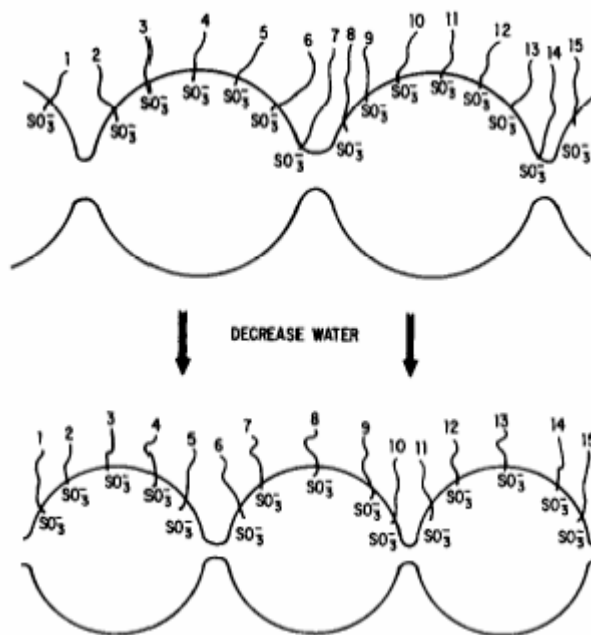


Figure 6 Schematic representation of redistribution of ion exchange sites which occurs on dehydration of the polymer [12].

Building on the model by Gierke, Yeager and Steck[13] described Nafion as consisting of three primary regions. The region breakdown is shown in Figure 7.

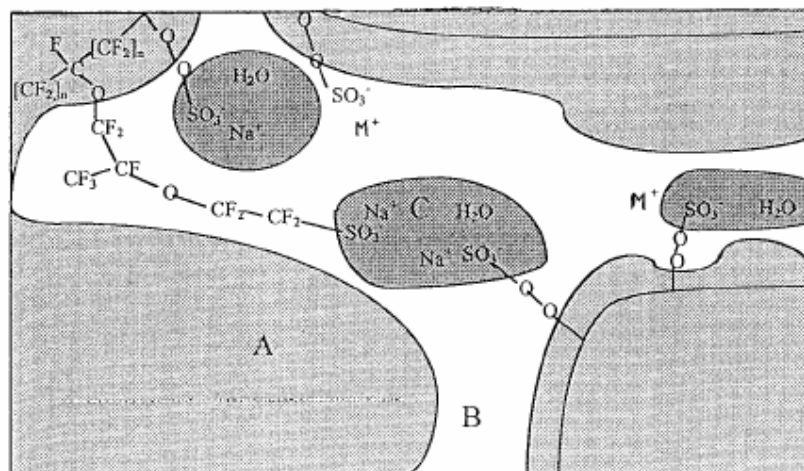


Figure 7 Three regions structural model for Nafion [13].

The labeled Region A consists of the TFE backbone material, in which there is some crystallinity. Region B is largely void space but also contains some side chain material, a little water, and some free sulfonate exchange sites. Region C contains the ion clusters, in which the sulfonate exchange sites, counterions, and about 75% of absorbed water exist. This is the most current model of the structure of Nafion.

3.4 Properties of Nafion

3.4.1 Equivalent Weight

The presence of ionic clusters greatly affects the mechanical and transport properties of the polymer. A property related to the ionic clusters is equivalent weight (EW). EW, a measure of the ionic concentration within an ionomer, relates to ionic conductivity, water uptake, and degree of swelling. The EW of a Nafion membrane can be expressed using the following equation:

$$EW = \frac{\text{grams of polymer}}{\text{moles of } \text{SO}_3^-}$$

At lower EW, the polymer loses mechanical integrity and will dissolve in water. At a high EW, the ionic groups are sufficiently dilute to afford too low an ionic conductivity for practical application. As the EW increases, the cluster diameter, number of ion exchange sites per cluster, and water per exchange site all decrease. Qualitatively, these trends may be understood by recognizing that the crystallinity and polymer stiffness increase with increasing EW.

3.4.2 Glass Transition

In an amorphous or semicrystalline polymer, the temperature at which it changes from being hard to being soft and flexible is known as the glass transition temperature, T_g . At higher temperatures, molecules, whether big or small, move around faster. This increased mobility is what permits the polymer to become soft and flexible. Above T_g , the polymer strands are able to move past each other more easily and therefore are more likely to move to new positions under an applied stress. On the other hand, a polymer below its T_g will not bend as easily. The following table lists the glass transition temperature of Nafion and also shows the T_g of Teflon for comparison.

	Dynamic Studies (ca. 1 Hz)	Calorimetric Studies ¹	Linear expansion by LVDT[14]
PTFE (Teflon)[15]	ca. 127		
(OH₂O/SO₃H)	111	104±1	122±11 ²
(3H₂O/SO₃H)³	109		

Table 1 Glass Transition temperature (in °C) of Nafion in its acid form as determined by different techniques[11]

¹ The temperature at which the slope of the lines changed (as determined by the intersection of the extrapolated straight line segments) was taken as the position of the transition or dispersion.

² Expansion coefficients above and below T_g were estimated as $8.2 \times 10^{-3} \text{ deg}^{-1}$ and $2.3 \times 10^{-3} \text{ deg}^{-1}$, respectively.

³ This water content was determined at the end of the experiment

It is important to note the glass transition temperature because of its role in the manufacture of membrane-electrode assemblies, discussed in section 4.

3.4.3 Mechanical Properties

The stress-strain curve is of principal interest for measuring the viscoelastic properties of a polymer. Young's modulus (also known as the storage or elastic modulus) is the slope of the initial linear or elastic region. It is a measure of how stiff the polymer is (i.e. how strongly the polymer resists stretching). The elastic modulus changes drastically with temperature. Two of the first to take such measurements were Yeo and Eisenberg[11]. Their results are shown in Figure 8.

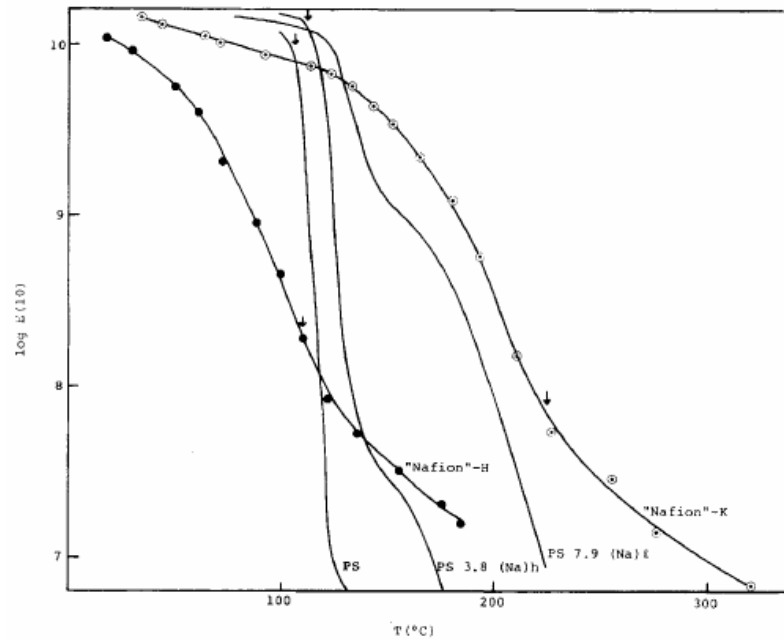


Figure 8 10-sec modulus (dynes/cm²) vs. temperature for Nafion-H, Nafion-K, PS, PS 3.8 (Na)h, and PS 7.9 (Na)l. Curves for styrene and two styrene ionomers are shown for comparison[11].

Figure 8 shows the modulus of Nafion in its acid (H) and salt (K) forms as a function of temperature. For both forms of Nafion, the value of the modulus at the glass transition

temperature (shown by the arrows) was two orders of magnitude lower than for the styrene ionomers. This discrepancy suggested an unusual packing effect and was one of the factors contributing to the conclusion that the ions in Nafion formed clusters.

The physical properties of Nafion at various water absorptions are shown in Table 2.

Property	Elastic modulus (MPa)	Tensile Strength (MPa)	% Elongation at Break
50% RH, 23°C	249	43 in MD, 32 in TD	225 in MD, 310 in TD
Water soaked, 23°C	114	34 in MD, 26 in TD	200 in MD, 275 in TD
Water soaked, 100°C	64	25 in MD, 24 in TD	180 in MD, 240 in TD

Table 2 Physical properties of Nafion membranes. MD stands for machined direction, TD for transverse direction, and RH for relative humidity [16]

As is evident from the above table, properties tend to decrease with increasing water content and temperature. Increasing the water content and/or temperature of Nafion makes the material softer and slightly weaker. The T_g of Nafion, the temperature at which the material becomes “rubbery”, is just above 100°C. As the Nafion nears its T_g , its modulus and tensile strength decrease because the polymer strands displace more easily in response to an applied stress.

Water acts as a plasticizer in Nafion, just as it does in Nylon. An increase in the amount of water absorbed would increase the size (but decrease the number) of the ionic clusters where much of the water accumulates. The increased water weakens the degree to which the ionic clusters act as cross-links, thereby decreasing the strength and modulus of the Nafion.

4. Membrane-Electrode Assembly (MEA)

4.1 Structure of the Electrode

The membrane-electrode assembly (MEA) consists of the electrode for the anode and cathode, and the membrane sandwiched in-between. A more detailed diagram of the fuel cell and the membrane-electrode interface is shown in Figure 9.

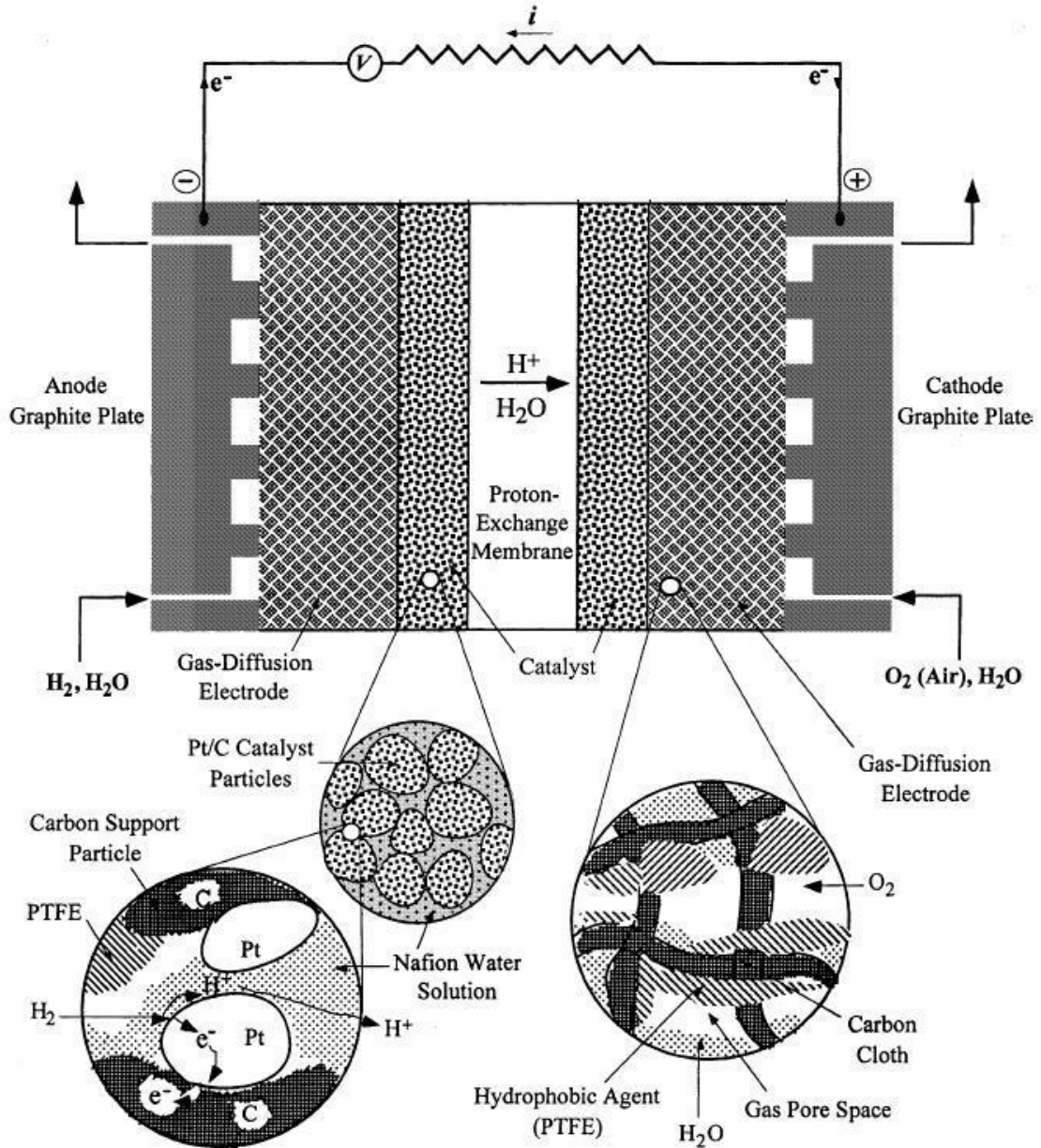


Figure 9 Schematic of the cross-section of a fuel cell consisting of the gas-diffusion electrodes, catalyst layers, and the polymer electrolyte membrane. The gas-diffusion backing fibers are coated with PTFE so as to be not flooded with water, while the catalyst layers comprise ionomer solution among Pt/C particles for proton transport[17].

The side of the electrode that neighbors the membrane contains the catalyst layer. The catalyst layer consists of small carbon particles with a very high surface area that are sputter-coated with the catalyst, Pt. The hydrogen fuel enters the anode and diffuses through the electrode until it reaches the catalyst. As shown in the lower left of Figure 9, once the hydrogen reaches the catalyst it is oxidized. The free electrons are conducted through the adjacent carbon particles whereas the hydrogen ions, or protons, travel to the cathode via the membrane. The simultaneous contact of the Pt, hydrogen gas, and Nafion is known as a three-phase interface and is critical for fuel cell operation; the more contact the membrane has with the catalyst particles, the greater the possibility for the existence of a three-phase interface. The typical fabrication procedure of an MEA is described below.

4.2 Procedure

The procedure for fabricating the MEA has not yet been standardized; consequently the manufacture of MEAs varies from group to group. However, a few things remain constant. In the press, the Nafion must be heated above its glass transition temperature before it is pushed into the membrane. A temperature of 140°C was decided upon because it is above the T_g of dry Nafion but not hot enough to destroy the membrane. The Nafion is soft and flexible at this temperature and should push into the porous openings of the electrode. A temperature of 160°C is to be avoided because the electrode might push all the way through the membrane. The MEA is placed in the press as it heats up to ensure that the membrane is dry when it is pressed. Wet Nafion is softer at lower temperatures and can therefore be pressed at a temperature lower than 140°C, but afterwards, when the water evaporates, the Nafion will contract and pull away from the electrode. A force rather than a

pressure is specified because force is easily read from the dial on the press. The side of the anode and cathode electrode that faces the membrane is painted with solubilized Nafion to maximize contact between the membrane and the catalyst. The Nafion and both electrodes are pressed for about one minute at 140°C and 1,000 lb_f.

5. Experimental Procedure

As discussed in section 1.2, we are trying to mimic a membrane-electrode interface in a fuel cell using a silicon wafer in place of an electrode. To produce an etched pattern on a silicon wafer, the first step is to come up with the desired pattern and transfer it to a chrome mask. Next, using ultraviolet (UV) light, the mask pattern can be copied to a silicon wafer using photolithography. Photolithography has six main steps: wafer preparation, photoresist application, softbaking, exposure, developing, and hard baking. These steps were performed in the clean room at Princeton University. After a photoresist mask is obtained, the pattern can be etched into the silicon wafer and the remaining photoresist removed. These silicon wafers served as the substrates against which the Nafion was pressed.

5.1 Creation of the Mask

Since it was desired to see a cross section of the interface between the polymer and the silicon wafer, the best shape for the features was determined to be long lines of varying widths. The exact length chosen was 2.5 cm, or about one inch, which accommodated for a small amount of error when fracturing the lines across the middle. The widths of the lines on the mask ranged from 2 to 50 microns, so as to mimic the porosity of the electrode. In addition to the line width, the space between the lines was also varied. In all, thirteen different line combinations comprised the master design. A description of each of the thirteen combinations is shown below in Table 3.

Line Combination #	Description of Pattern
1	1" long trenches of widths 2, 5, 10, 15, 20, 30, 40, and 50 microns (μm) each spaced by 50 μm . This combination is repeated 3 times.
2	Eight 1" long trenches that are 2 μm wide and separated by 2 μm . This combination is repeated 3 times.
3	Eight 1" long trenches that are 2 μm wide and separated by 5 μm . This combination is repeated 3 times.
4	Eight 1" long trenches that are 2 μm wide and separated by 10 μm . This combination is repeated 3 times.
5	Eight 1" long trenches that are 5 μm wide and separated by 2 μm . This combination is repeated 3 times.
6	Eight 1" long trenches that are 5 μm wide and separated by 5 μm . This combination is repeated 3 times.
7	Eight 1" long trenches that are 5 μm wide and separated by 10 μm . This combination is repeated 3 times.
8	Eight 1" long trenches that are 10 μm wide and separated by 2 μm . This combination is repeated 3 times.
9	Eight 1" long trenches that are 10 μm wide and separated by 5 μm . This combination is repeated 3 times.
10	Eight 1" long trenches that are 10 μm wide and separated by 10 μm . This combination is repeated 3 times.
11	Eight 1" long trenches that are 15 μm wide and separated by 2 μm . This combination is repeated 3 times.
12	Eight 1" long trenches that are 15 μm wide and separated by 5 μm . This combination is repeated 3 times.
13	Eight 1" long trenches that are 15 μm wide and separated by 10 μm . This combination is repeated 3 times.

Table 3 Descriptions of the thirteen different line combinations that appear on the mask to be transferred to the silicon wafer.

As mentioned in Table 3, each combination was repeated 3 times. The separation between these repeats and also between the different line combinations was 50 μm .

After the mask design was established, the mask had to be created. The design of the mask was transferred to the computer using AutoCAD design software. The mask was fabricated using the Heidelberg DWL66 Laser writer in the clean room at Princeton University⁴. About 17 hours were required to transfer the pattern from the computer to the mask using the 4mm writehead. Afterwards, the exposed chrome was lifted off by sonication and the mask was inspected under the optical microscope.

⁴ Courtesy of Helena Gleskova.

5.2 Photolithography

The silicon wafers⁵ used were 3” diameter (100) test grade wafers. Before use, the wafers were rinsed with acetone and isopropanol, dried with nitrogen, and baked on a hot plate for 15+ minutes at 110°C to dehydrate. After the wafers were cleaned and baked, a layer of hexamethyldisilazane (HMDS) was spun on to promote adhesion between the wafer and the photoresist. A layer of AZ5214 photoresist was spun on top of the HMDS (shown in Figure 10). Immediately after the application of the photoresist, the wafer was soft baked on a hot plate for one minute at 95°C. Soft baking removes most of the remaining solvent from the photoresist film, thereby making it denser.

Following this baking, the wafers were exposed to UV light through the mask previously created using the Karl Suss MA6 mask aligner. AZ5214 is a positive photoresist, which means that exposure to UV light causes the photoresist to break down and become soluble in the developer. After an exposure time of 25 seconds, the wafer was developed in a 50:50 mixture of DI water and MIF312 for 25-35 seconds to remove the exposed photoresist. The developing solution was rinsed off using DI water, and the wafers were dried with nitrogen and inspected under an optical microscope. A schematic of the photoresist after development is shown in Figure 10b.

⁵ Obtained from University Wafers, P-type doping, any resistivity, 380±20 µm thick, one side polished



Figure 10a Schematic showing layer of photoresist on top of Silicon wafer



Figure 10b Schematic showing patterning in photoresist after developing. The developer washes away the photoresist exposed to UV light, revealing the silicon wafer beneath.

The optical microscope was used to determine if the photoresist was completely removed and all the patterns were visible. If the patterning was satisfactory, the wafers were hard baked on a hot plate for 6 minutes at 110°C. Hard baking improves the stability, adhesion, and chemical resistance of the photoresist and is a necessary step before etching. If errors existed in the photoresist, it was rinsed off using acetone and isopropanol and the photolithography process was repeated.

5.3 Reactive Ion Etching (RIE)

There are two main ways to etch silicon: dry and wet etching. In dry etching, the wafer is placed in a chamber into which gases are introduced. A plasma phase is obtained using an RF power source, breaking the gas molecules into ions. The ions chemically react with the surface of the material to form a second gaseous material, thereby removing solid material from the surface. The ions can also accelerate towards the material and knock atoms off without reacting with them. Thus there is a chemical and physical part of RIE. Wet etching involves immersing the wafer in a liquid solution of chemicals to etch away the material. It is a simple, easy, and relatively quick process. However, (100) silicon exhibits anisotropic etching (different etch rates in different directions) when immersed in KOH. The result of an anisotropic etch in KOH is an inverted pyramid shape whereas straight

sidewalls can be obtained with RIE. For this reason, and also due to the photoresist's inability to remain on the silicon wafer in KOH, the RIE method was chosen to etch silicon.

RIE was performed using the Plasmatherm 720 in the clean room at Princeton University. The gases used were SF_6 and CCl_2F_2 with flow rates of 60 and 20 sccm respectively. Other conditions specified included pressure (100 mTorr), temperature (25°C), and power (100 Watts). This recipe produced an etch rate of about $1.14\text{ }\mu\text{m}$ in 5 minutes. However, the etch rate in RIE is not linear with respect to time, so this rate is just an approximate value. The samples were etched for 25 minutes and obtained a depth of about $5\text{ }\mu\text{m}$. The photoresist mask was removed by multiple rinses in acetone and isopropanol. A schematic of the etching process is shown in Figure 11a and 11b.



Figure 11a Schematic of photoresist and silicon wafer after RIE. The photoresist acts as a mask so only the exposed areas of the silicon are etched.



Figure 11b Schematic of the final etched silicon wafer after the photoresist is removed.

As shown in Figure 11a, during an RIE etch only the exposed areas of the silicon wafer are etched; the hard-baked photoresist acts as a mask. Thus, only the desired pattern is etched into the wafer and the photoresist is easily removed after etching.

5.4 Hot Pressing

Since the samples were ultimately going to be viewed in the Scanning Electron Microscope (SEM), they needed to be cut into smaller pieces. The master design discussed

in section 5.1 was repeated 9 times on one silicon wafer. Each design was about one centimeter wide and 2.5 centimeters long. The silicon wafer was cut using a diamond scribe into pieces that only contained the master pattern.

A piece of 1110 Nafion (about 250 microns thick) was cleaned by boiling in hydrogen peroxide (3%) for 1 hour, rinsing in boiling de-ionized (DI) water for 1 hour, boiling in 1.0M H_2SO_4 for 1 hour, and then rinsing again in boiling DI water for 1 hour. It was then cut into 1 cm by 2.5 cm pieces to be placed on top of the silicon substrates. The samples were prepared as to replicate the preparation of an electrode assembly for a normal polymer electrolyte fuel cell. Thus, the Nafion membrane was placed one on top of the silicon and pressed in a hot press. A diagram showing the layers of material is shown in Figure 12.

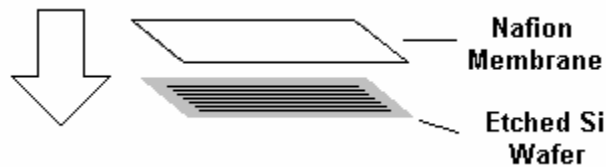


Figure 12 Diagram showing sequence of materials pressed on top of each other. The lines etched in the Si wafer are designed to mimic the spacing in the electrode pressed on the top side of the Nafion.

The gauge of the hot press measured a force rather than a pressure, so 2000 lb_f was chosen because it was the smallest force that could be read on the gauge.

5.4.1 Temperature Selection

Samples were pressed at a wide range of temperatures in order to find the temperature at which Nafion deformed most completely into the small spaces. A temperature of 140°C was chosen since MEAs are normally fabricated at this temperature.

Lower temperatures such as 50 and 60°C were also tried, as the normal operation of PEMFCs is between 50 and 90°C (section 2.3). Samples were also pressed at temperatures in between (90, 100, and 110°C) in order view Nafion deformation around its glass transition temperature. Table 4 below shows the conditions under which the samples were prepared.

Sample	ETCH COND		PRESS COND		
	exp time	etch time	Nafion	Temp	Dry/Amb/Wet
1	25 sec	30 min	1110	50°C	Amb
2	25 sec	30 min	1110	50°C	Amb
3	40 sec	30 min	1110	50°C	Wet
4	40 sec	30 min	1110	140°C	Amb
5	25 sec	25 min	1110	140°C	Amb
6	25 sec	25 min	1110	140°C	Wet
7	25 sec	30 min	1110	50°C	Amb
8	25 sec	30 min	1110	50°C	Amb
9-10	25 sec	25 min	1110	34°C	Wet
11-12	25 sec	25 min	1110	60°C	Wet
13-14	25 sec	25 min	1110	100°C	Wet
15-16	25 sec	25 min	1110	140°C	Amb
17-19	25 sec	25 min	1110	100°C	Amb
20-21	25 sec	25 min	1110	60°C	Amb
22-27	25 sec	25 min	1112	90°C	Amb
28-35	25 sec	25 min	1112	110°C	Amb

Table 4 Conditions under which each sample was etched and pressed.
All samples were pressed at a force of 2,000 lb_f and a time of 90 seconds.

The conditions on the left of Table 4 describe the conditions of the photolithography and etch. The exposure time refers to how long the photoresist was exposed to UV light in the mask aligner. The difference in exposure time simply signifies that a slightly different recipe was used to pattern the photoresist. This makes no difference in the etch of the silicon

wafer, but was noted just to be thorough. The etch time indicates how long the sample was exposed to reactive ion etching. The depth was measured using a profilometer; etching for 25 minutes corresponded to depth of $\sim 5\text{ }\mu\text{m}$.

As mentioned in section 2.3, the Nafion membrane in a PEMFC must be humidified to function. Since Nafion swells as its water content increases, it was important to explore the effect of water content on the deformation of Nafion. The “wet” samples in Table 4 were boiled in DI water for at least ten minutes, then immediately removed and placed on the silicon substrate in the press. The difficulties observing the wet samples are described below. All samples were pressed the night before they were examined in the SEM and left at room temperature overnight.

5.5 Difficulties in Sample Preparation

5.5.1 Wet Samples

Any sample hydrated above the ambient humidity level was not able to be tested. After wet samples were removed from the press, the water in it started to evaporate and the Nafion shrunk and ultimately pulled away from the piece of silicon. As more time passed, the membrane curled up, so it was not even possible to examine a flat piece of the polymer. This problem was evident at temperatures through 100°C . However, at 140°C , the Nafion remained attached to the silicon. Since the sample was warmed in the press up to 140°C , all of the water would have evaporated before the pressure was applied. Thus, a wet sample pressed at 140°C behaved the same as a dry sample.

5.5.2 Fracturing in Liquid Nitrogen

In order to obtain a cross section of the samples, they were freeze-fractured. The back of the silicon piece was scored with a diamond scribe and the entire sample was placed in liquid nitrogen for 1-2 minutes before fracturing. Unfortunately, the silicon-polymer arrangement did not snap in the liquid nitrogen as hoped. Instead, only the silicon wafer fractured. Fortunately, the Nafion still retained the pattern of trenches without the wafer. Ideally, a new method for sample preparation should be invented to ensure the Nafion/silicon interface remains intact.

6. Results and Discussion

Before the samples were placed in the SEM, they were sputter coated with 4 nm of Iridium. As mentioned in section 5.5.2, sample preparation was very difficult. It was extremely hard to fracture the silicon and Nafion together. Hence, in many of the pictures obtained the Nafion is not flush against the silicon wafer. Image 1 shows one of the more successful samples: the Nafion remained very close to the silicon wafer.

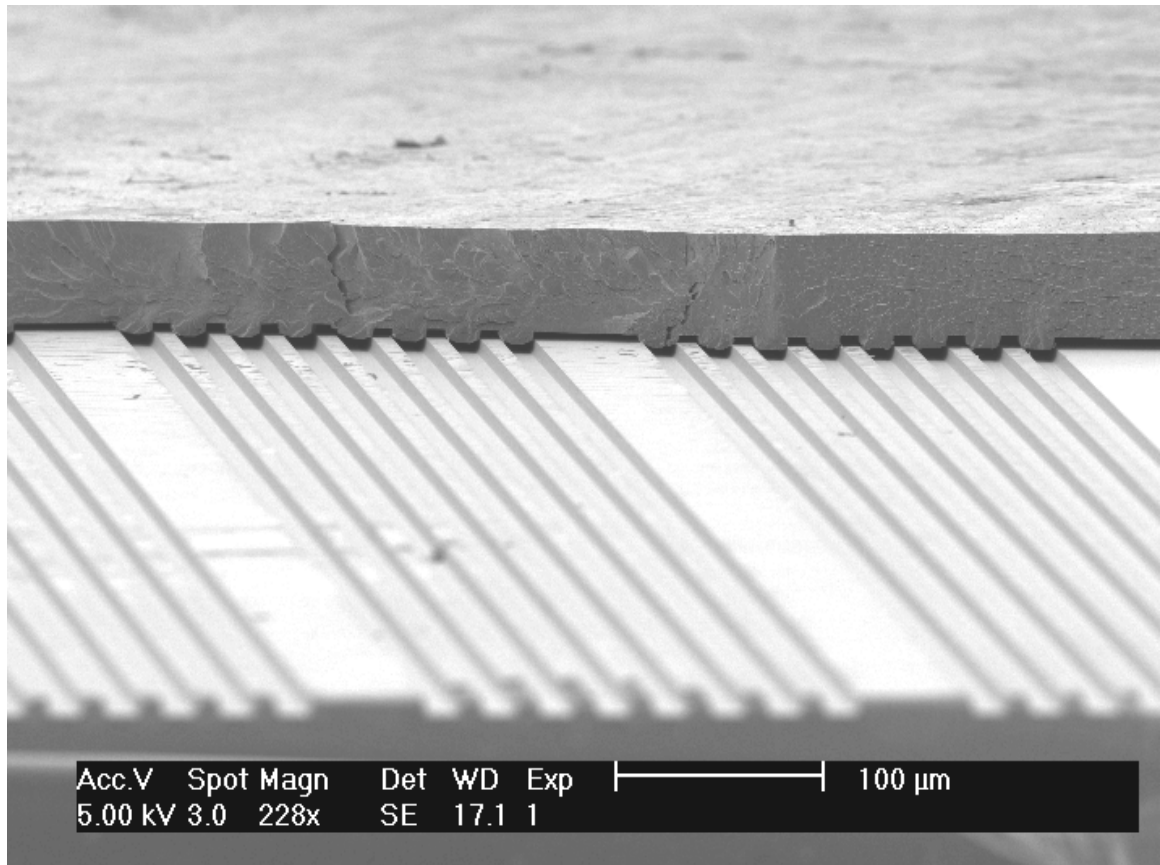


**Image 1 Overview of how Nafion-silicon complex appears in the SEM.
The Nafion is on the top, the etched silicon wafer is on the bottom.**

The rest of the pictures shown in this section offer a more magnified view of the interface between the Nafion and the silicon. However, Image 1 provides a larger picture so the reader is aware of what he/she is looking at.

6.1 The Effect of Temperature

6.1.1 At 140 degrees Celsius

The glass transition temperature of dry Nafion in its acid form is between 100 and 110°C. Thus, Nafion pressed at 140°C is well above its T_g and should be soft and moldable.

Image 2 below shows the interface of Nafion and silicon pressed at 140°C.

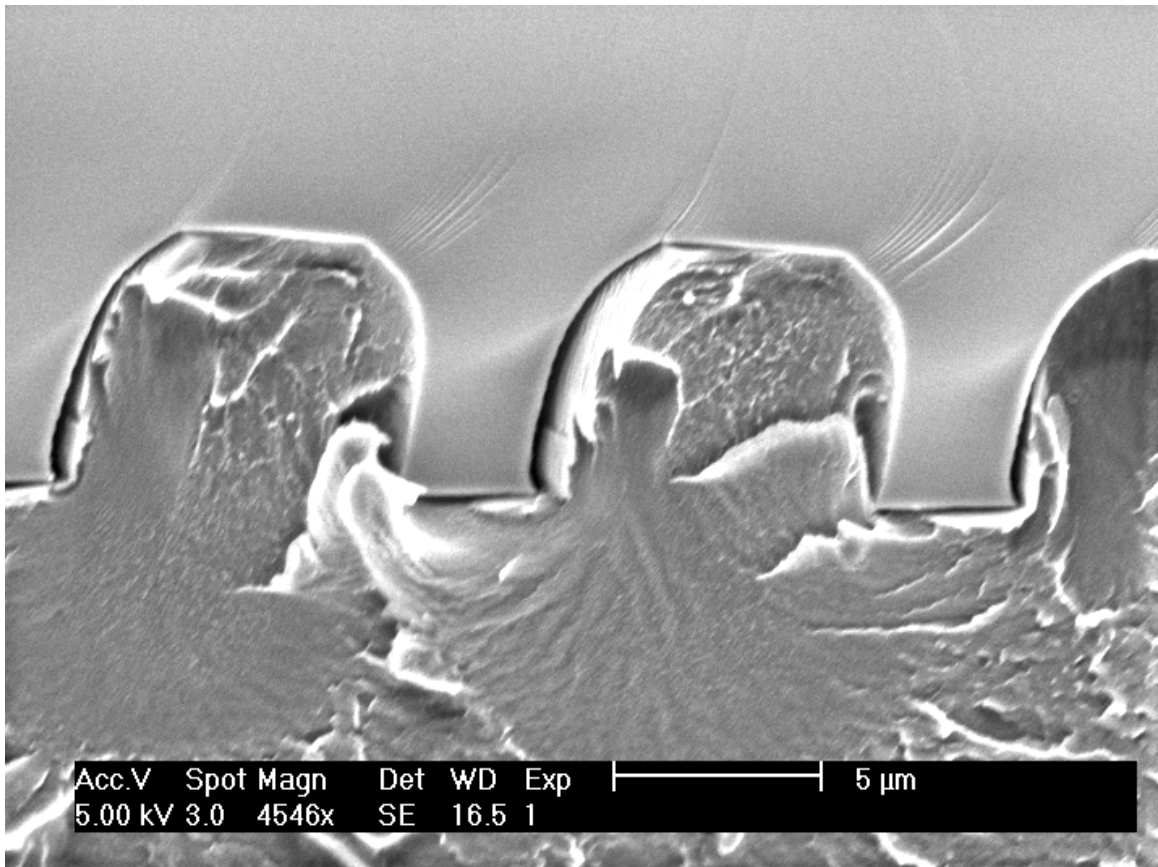


Image 2 - SEM image of sample 4 (140°C). Nafion completely pressed into the 5 μm feature. Nafion on bottom, silicon wafer on top.

At 140°C the polymer completely extruded into all features of width 5 μm and larger. The width of the actual feature is slightly larger than 5 μm because the etch enlarged the feature. For the features that were 2 μm wide, a different phenomenon was observed. Two micron features are shown in Image 3.

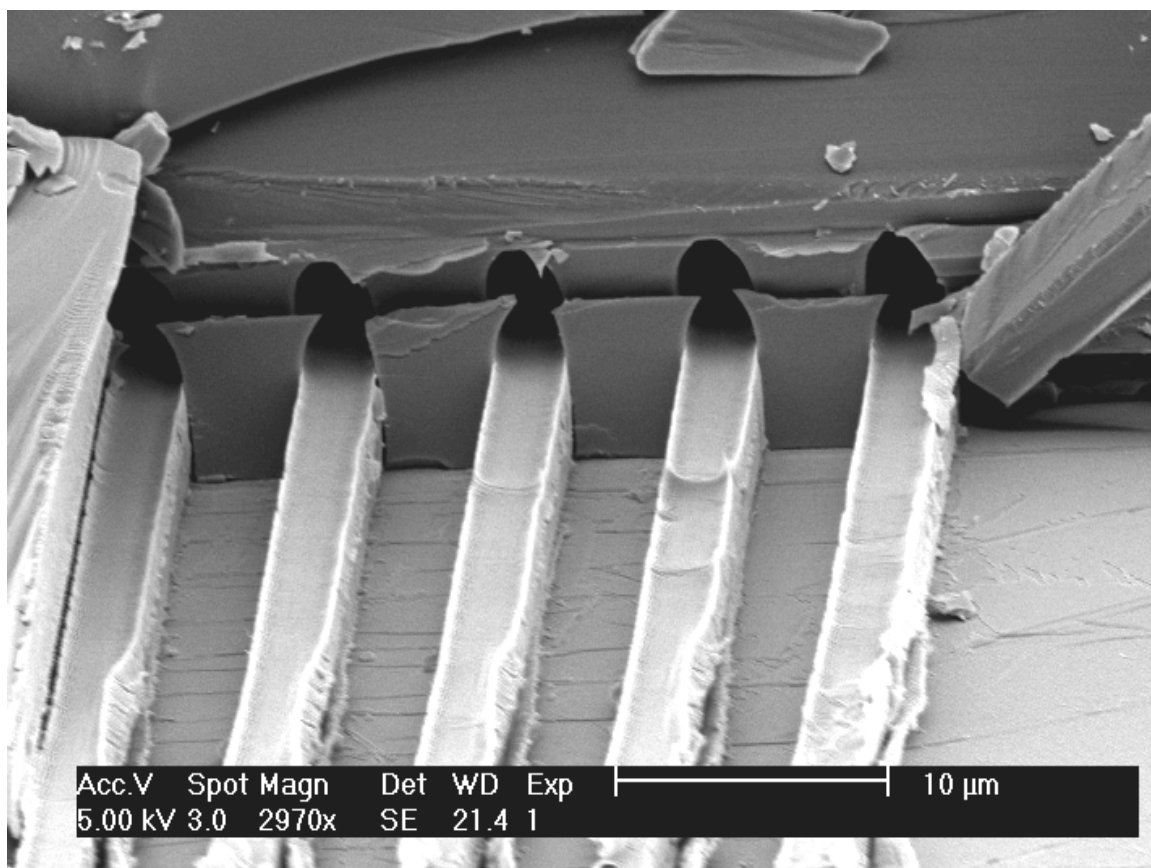


Image 3 SEM image of sample 15 (140C). Nafion did not press all the way into the 2 μm feature. Nafion is on the bottom, silicon is on the top.

The failure to press completely into the 2 μm features was evident at all temperatures.

However, at 140°C, the Nafion in the 2 μm features exhibited a curvature that was exactly the opposite of the curvature of the feature in the silicon. An explanation for this behavior is offered in section 6.3.

6.1.2 At 60 degrees Celsius

At a temperature of 60°C, the Nafion is well below its T_g . As such, it was expected to see less deformation than at 140°C. Image 4 shows the deformation observed at 60°C.

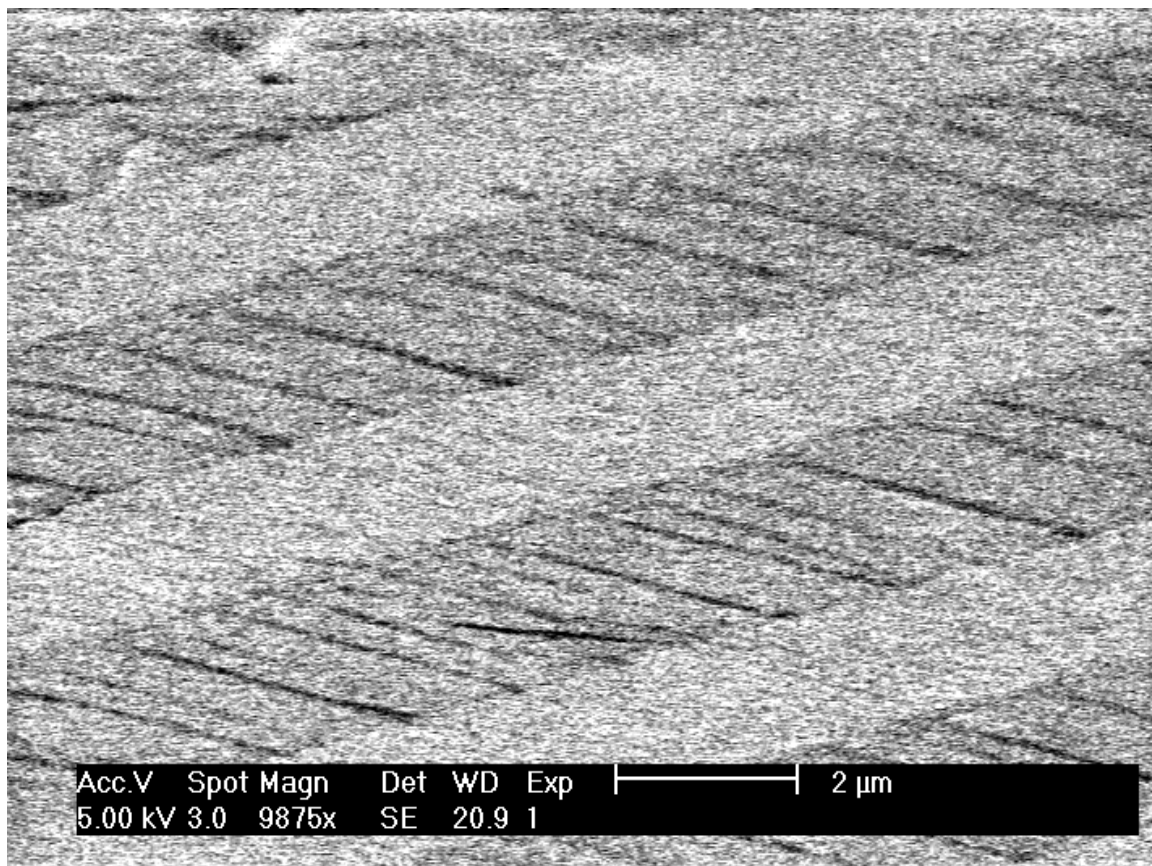


Image 4 SEM image of sample 20 (60C). Nafion exhibited no deformation.

Only Nafion is present in the image above because it had pulled away from the silicon wafer it was pressed against. The image of the silicon wafer is present on the Nafion but there are no raised features of any size.

In contrast with the Nafion pressed at 140°C (Image 2), the Nafion at 60°C (Image 4) appears to have a much more rigid structure. Not only did it not deform into any features, but there are also many cracks on the surface where the Nafion should have pressed into the silicon. The cracks are evidence of brittle fracture. This confirms that the Nafion was in a glassy state when pressed.

6.2 Behavior Around the Glass Transition Temperature

It is clear that the temperature at which the Nafion is pressed significantly affects the deformation of the polymer. At a temperature greater than its T_g , the Nafion easily deforms into almost all the features on the silicon wafer, whereas at a temperature greatly below its T_g , no deformation is observed. Thus, the behavior of Nafion at temperatures closer to its T_g was analyzed. The deformation of Nafion into 2 μm features at 90°C is shown in Image 5.

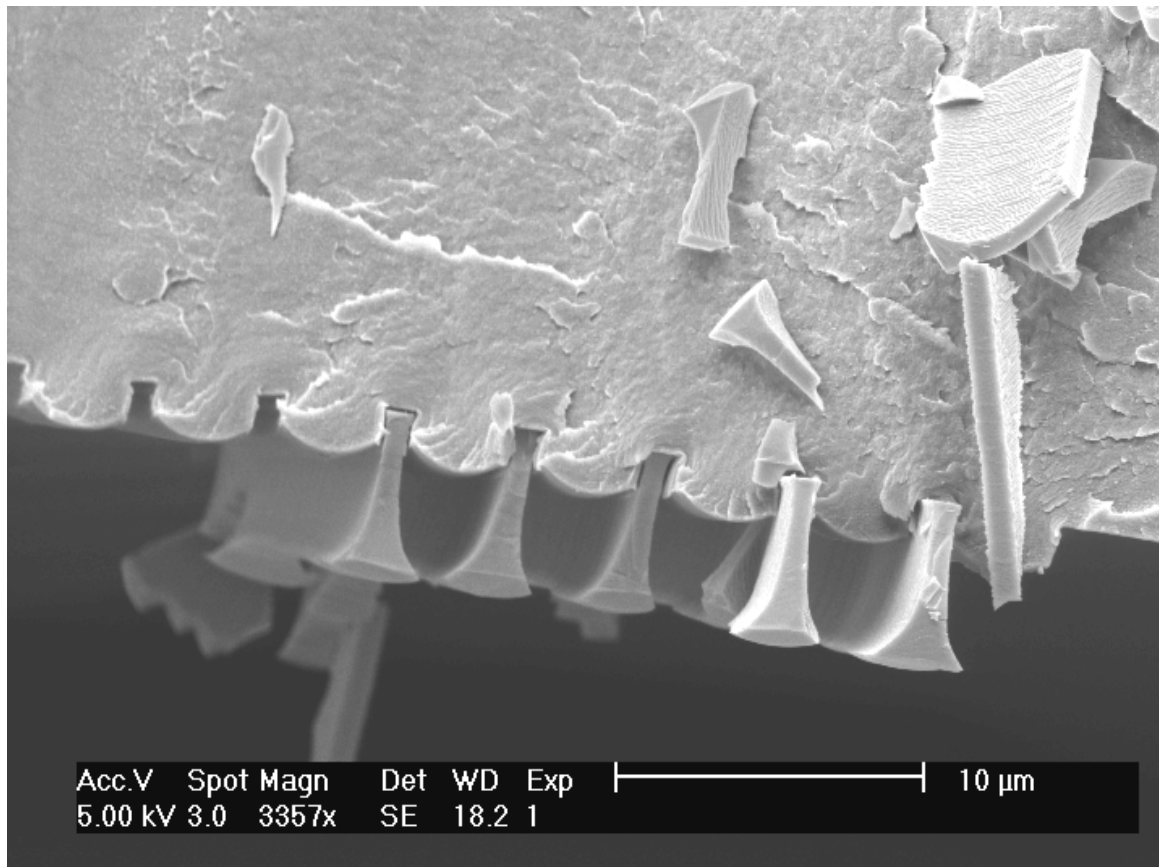


Image 5 SEM image of sample 27 (90C). Nafion deformation into 2 micron features. Nafion on top with pieces of the trench walls stuck in the Nafion.

This piece of Nafion had pulled away from the silicon wafer, but from the pieces of the wafer that remained it is evident that the Nafion did not press all the way into the 2 μm features. The curvature of the Nafion in these features is the same as the bottom of the

trench, but is the opposite of what is observed at 140°C. The reason for this is discussed in section 6.3.

Unlike the Nafion pressed at 140°C, at 90°C the Nafion did not completely deform into the larger features. A 15 μm wide feature at 90°C is shown in Image 6.

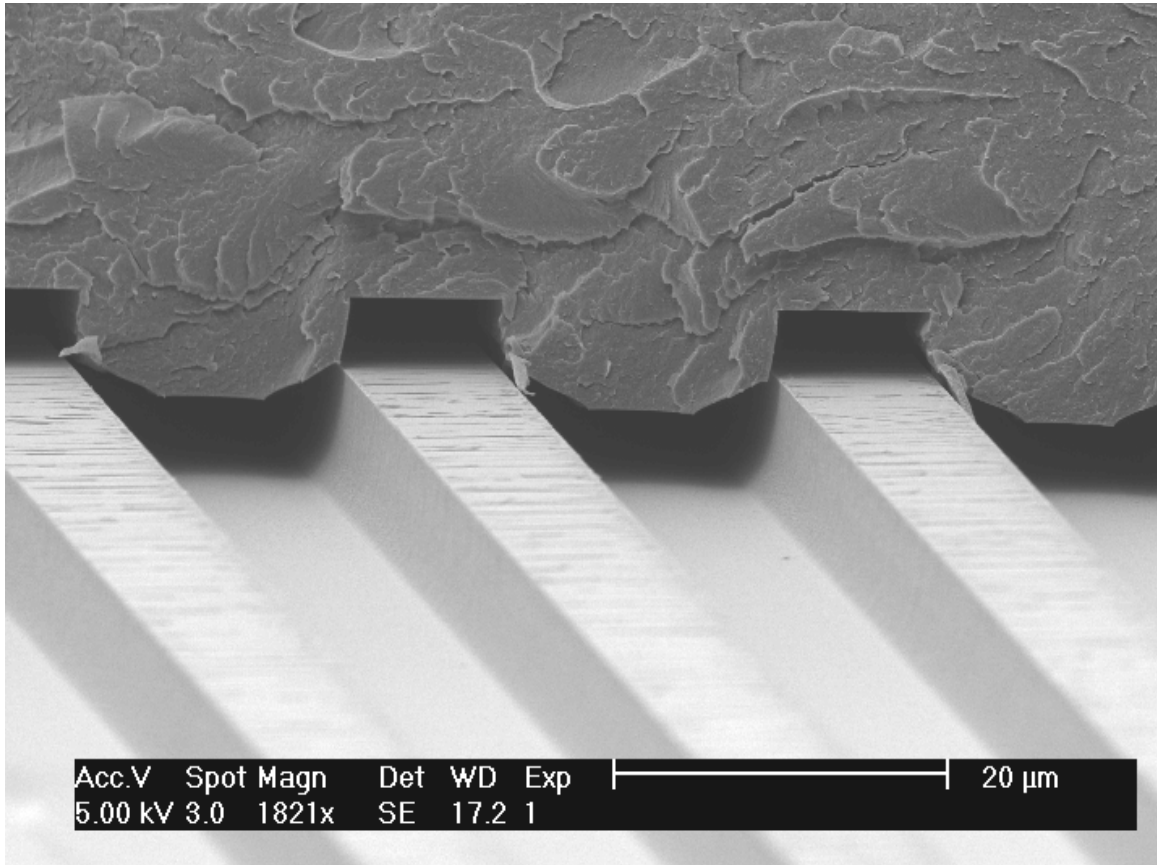


Image 6 SEM image of sample 27 (90C). The Nafion did not completely press into the 15 micron feature. Nafion is on the top, silicon is on the bottom.

From Image 6 it is obvious that the Nafion did not completely press into the trench because the Nafion did not take on the shape of the entire trench. The part that touched the bottom formed a flat surface but the corners are angled from the part that reached the bottom to the part that touched the side walls.

At widths less than 15 μm , no part of the Nafion touched the bottom of the trench, which confirms that 90°C is about the temperature when Nafion is just starting to become

soft enough to be pushed into the features on the silicon wafer. At 110°C, just 20 degrees higher, the Nafion once again deformed completely into all the features except the 2 micron sized ones.

6.2.1 Stress features

The deformation at 110°C was identical to that observed at 140°C, except the Nafion in the 2 μm features exhibited less of a reverse curvature. At 90°C, the Nafion was not soft enough to completely deform into all of the features and the Nafion in the 2 μm features did not have a reverse curvature. At 100°C, a temperature in between, very interesting behavior was observed. First, the Nafion deformed into all features with widths of 5 μm or greater. However, no reverse curvature was evident for the Nafion in the 2 μm features. Furthermore, a cross section showed evidence of glassy behavior in the Nafion. Image 7 demonstrates this behavior.

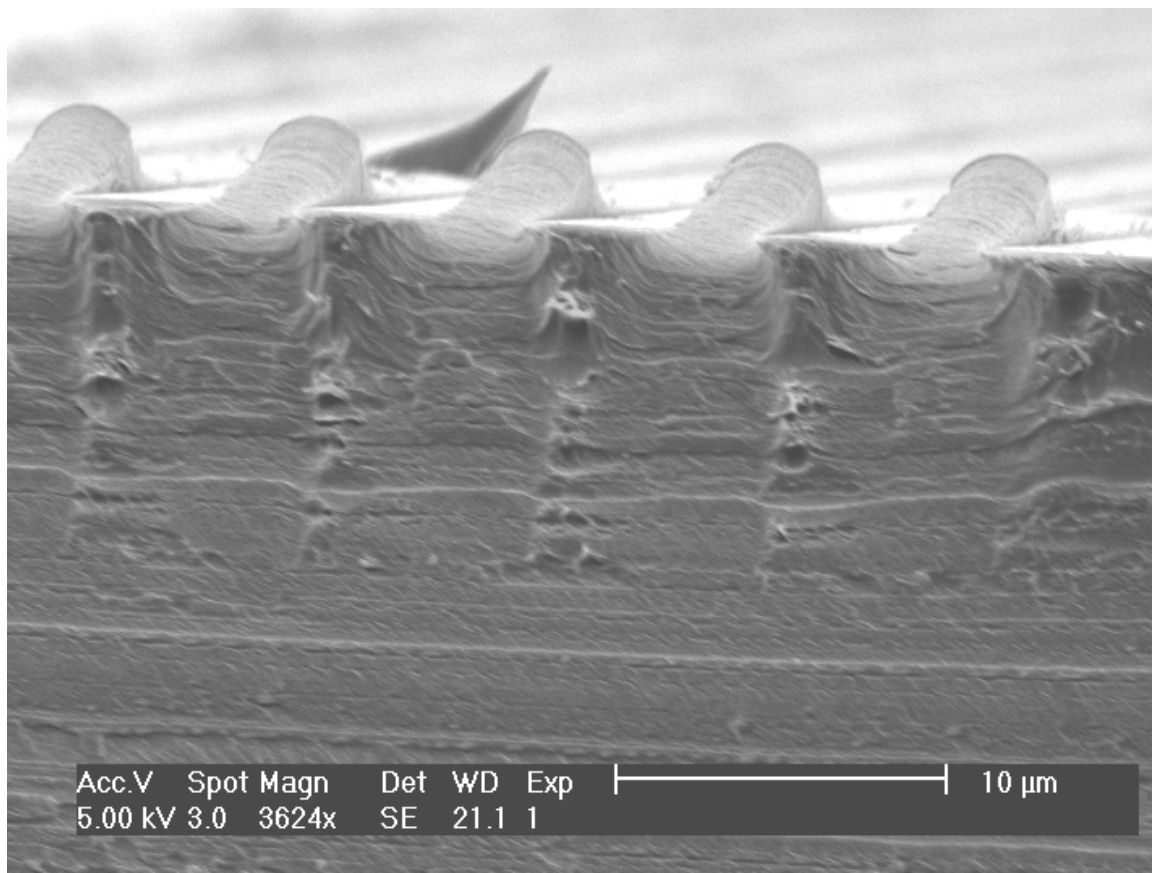


Image 7 SEM image of sample 17 (100C). Glassy behavior evident in the Nafion. Only Nafion is shown.

As shown above, striations are apparent in the Nafion to a depth of $\sim 10\ \mu\text{m}$. The Nafion itself also appears to have a much more layered structure than it does at 90°C or at higher temperatures.

It is interesting that these striations appear at 100°C but not at 90°C . At 90°C , a temperature 10 degrees lower, the polymer should be even more “glassy.” Nevertheless, as Image 6 shows, the polymer does not display the same striations.

It is believed that the polymer is still in a glassy state at both 90 and 100°C . However, as mentioned before, at 100°C the Nafion deformed completely into all features. Thus, the force at which the sample was pressed was more than was necessary to distort the

Nafion. This extra applied force might have caused the striations and layered structure to form in the polymer.

Another reason for this behavior is the thickness of the membrane. Due to the difficulty of sample preparation, a thinner Nafion membrane was used in the later samples (#22-35), which includes those pressed at 90°C, because it fractured more easily in liquid nitrogen. However, the thinner membrane was only $\sim 50\text{ }\mu\text{m}$ thick and this thickness, perhaps, was not large enough for the Nafion to exhibit the same stress behavior as was observed in the thicker membrane.

6.3 Nafion Deformation in 2 micron Features

As mentioned in section 6.1.1, Nafion did not completely press into a two micron feature at any temperature. However, at 140°C the polymer exhibited a reverse curvature in the features. A close-up view of this behavior is shown in Image 8.

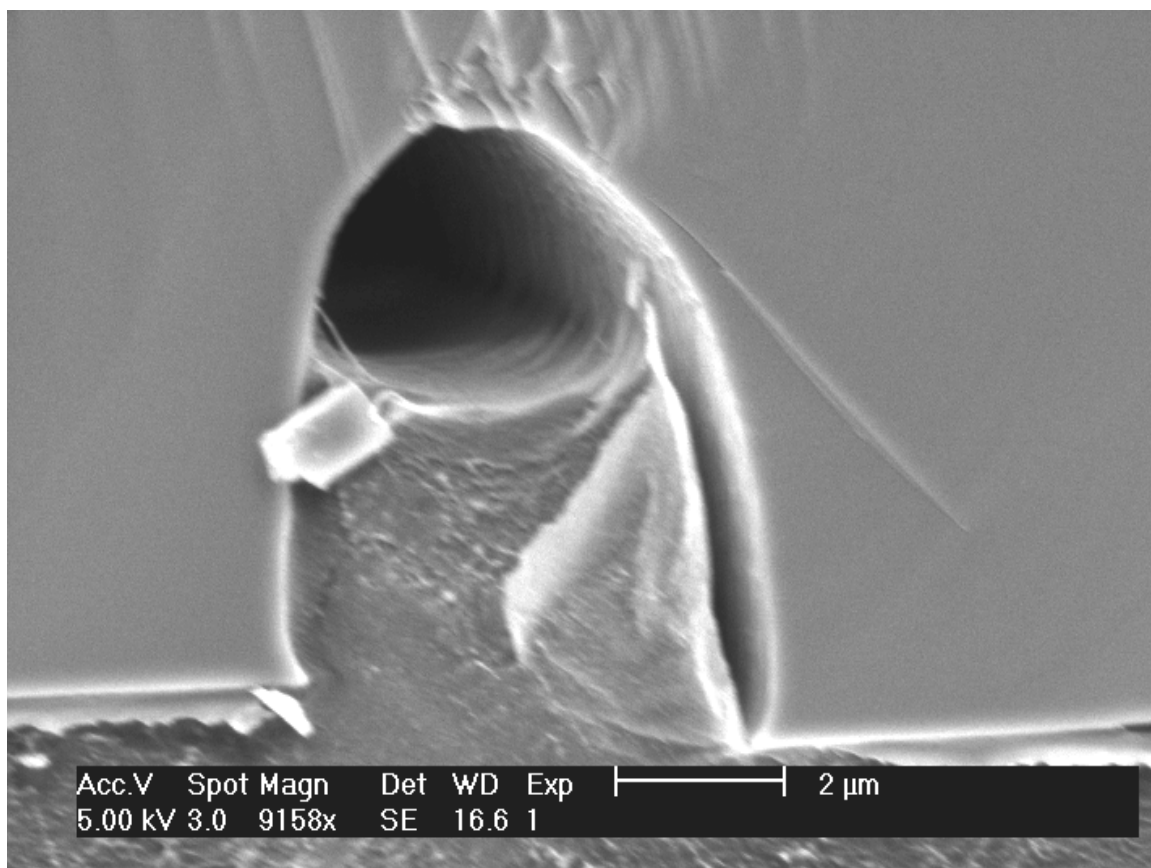


Image 8 SEM Image of sample 4 (140C): the reverse curvature of Nafion in a 2 micron feature. Nafion is on the bottom, silicon is on the top.

The edges of the Nafion appear to have crawled up the wall of the silicon. At first glance it looks as though an air bubble may have formed – especially because the curvature of the Nafion is uniform. If air were trapped in the small feature, the compression of the air would cause the Nafion to deform around it and form a rounded surface. However, “air bubbles” are not present in features of any other size.

An alternate explanation involves surface energy. At 140°C, which is significantly above the glass transition temperature, the pictures suggest that a wetting phenomenon may have occurred, just as water wets a capillary tube. Nafion is an ionomer that has a reverse micellar structure where the hydrophilic sulfonic acid groups form ionic clusters in which water aggregates when the material is hydrated. To minimize surface energy, these

hydrophilic groups should neighbor the silicon surface. At 140°C the polymer might have enough energy to rearrange itself so that the surface bordering the trench wall is hydrophilic and thus wets the surface of the silicon.

The time required for the rearrangement of the ionomer is highly dependent on temperature. Figure 13 relates the diffusion coefficient, D , to the Brownian displacement, x , and the time t .

$$2tD = x^2$$

Figure 13 Einstein's equation relating the diffusion coefficient D to the Brownian displacement x and time t [18].

Temperature enters into the diffusion coefficient, which is greater at higher temperatures. Unfortunately, the relation in Figure 13 describes the diffusion of single atoms rather than long polymer chains and thus cannot be directly applied in this thesis. However, it can still indicate two useful relations. First, at higher temperatures, the diffusion coefficient is greater and thus molecules will diffuse more quickly. Our results appear to support this claim because the Nafion only rearranged its surface at higher temperatures. Second, at longer times the molecules will travel greater distances. On the small length scale of this experiment, however, temperature will have a much greater effect on the polymer's ability to rearrange than time.

At temperatures lower than 140°C, the Nafion also failed to deform completely into the trench, but did not exhibit the same reverse curvature. At these lower temperatures, it is believed that the polymer did not have enough energy to rearrange to have a hydrophilic surface neighboring the silicon, preventing the same wetting phenomenon from occurring. Rather, the viscosity of the Nafion governed the deformation into the trench.

Viscosity can be qualitatively described as a material's resistance to flow. Parameters such as temperature, pressure, and molecular weight (MW) affect a polymer's viscosity.

Here only temperature effects are considered because effects of pressure are usually noticeable only at high pressures (hundreds of atmospheres)[19] and the MW of the Nafion was not varied throughout the experiment. The effect of temperature on zero-shear viscosity, η_0 , is shown by the Williams-Landel-Ferry (WLF) equation in Figure 14.

$$\log_{10} \frac{\eta_0(T)}{\eta_0(T^*)} = \frac{-C_1(T - T^*)}{C_2 + (T - T^*)}$$

Figure 14 WLF equation depicting effect of temperature on zero-shear viscosity

Zero-shear viscosity is simply the viscosity measured at low shear rates (or stresses) and from now on will simply be referred to as viscosity unless otherwise mentioned. The WLF equation relates the viscosity at the desired temperature to a reference temperature, T^* . If the glass transition temperature is used as the reference temperature, then C_1 and C_2 become universal constants with $C_1 = 17.44$ and $C_2 = 51.6$ (with temperature in Kelvin). A graph demonstrating the relationship between the ratio of viscosities and temperature is shown in Figure 15.

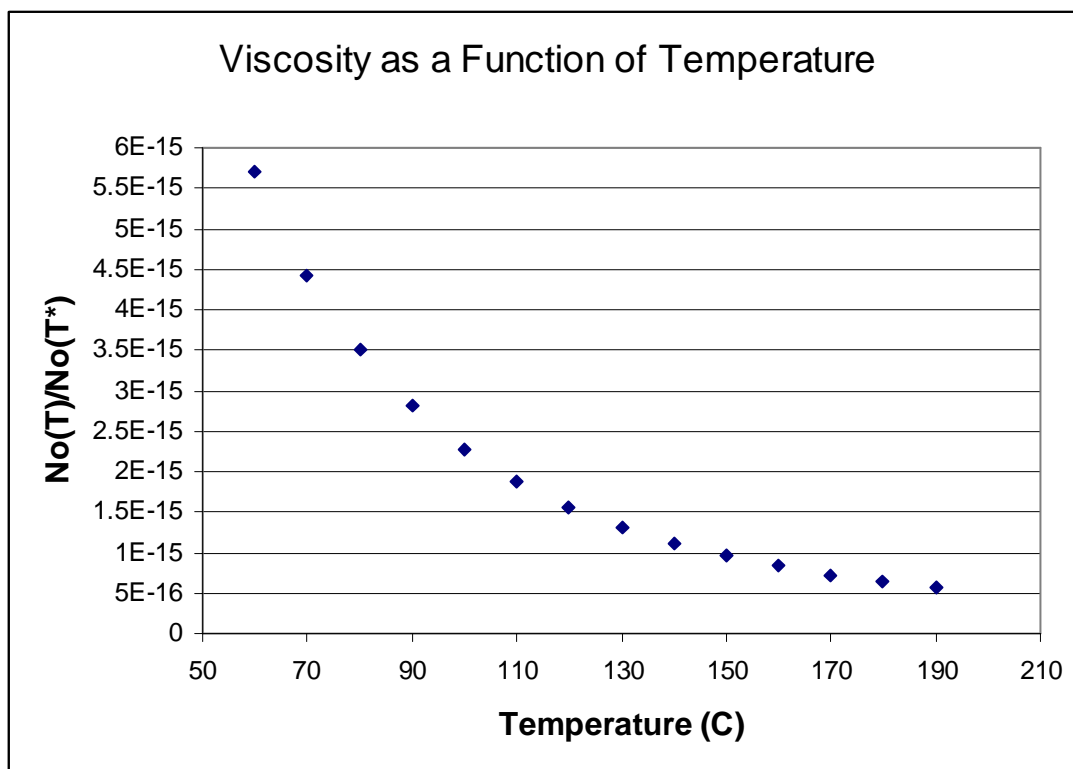


Figure 15 A plot of Temperature vs. viscosity ratio using the WLF equation.

While Figure 15 supplies no absolute values for viscosity, it does accurately demonstrate that viscosity is a strong function of temperature. The quantity $\frac{\eta_0(T)}{\eta_0(T^*)}$ is plotted on the y-axis.

Since the viscosity at the reference temperature T^* remains constant, Figure 15 shows that viscosity decreases as temperature increases. The WLF equation is applicable for use with temperatures that are in the range $T_g < T < T_g + 100^\circ\text{C}$. Below T_g , the viscosity will increase at an even greater rate than shown in Figure 15, so the values shown between 60 and 100°C can be thought of as a lower limit. It makes sense, then, that samples pressed at 60°C did not deform at all because their viscosity was at least 5 times that of the viscosity at 140°C . Similarly, samples pressed at 90, 100, and 110°C had viscosities that were at least 2.5, 2.0, and 1.8 times greater than that at 140°C , respectively.

7. Conclusions

7.1 Importance for Fuel Cell Operation

This thesis explored the deformation of Nafion into small features and the effect of temperature on this deformation. The motivation was based on an observation of a jump in current when decreasing a fuel cell's load, thereby increasing the amount of water produced. Increased water production causes Nafion to swell in a confined area and therefore puts stress on the membrane. Figure 16 demonstrates how the Nafion pressed on the silicon compares to Nafion pressed into an electrode.

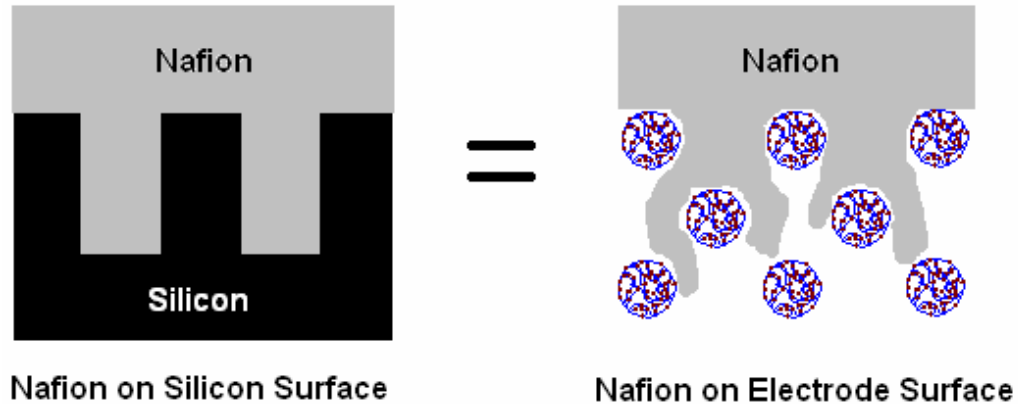


**Figure 16 (Left) Cross section of Nafion pressed onto a silicon wafer.
(Right) Cross section of Nafion pressed onto an electrode.**

The spheres shown on the right in Figure 16 are the high surface area carbon particles ($\sim 1 \mu\text{m}$) coated with Pt catalyst particles ($\sim 5 \text{ nm}$) that border the Nafion membrane in a fuel cell. The SEM images of the cross section of the Nafion/silicon laminate revealed that the Nafion remained completely pressed into the features etched on the silicon wafer even at room temperature. Since the Nafion was pressed onto the silicon at the same conditions at which an MEA is fabricated, it is likely the Nafion also remains deformed into the porous electrode surface. If this is true, then when Nafion swells due to increased water content, its

expansion from side to side is probably a more significant factor than its expansion deeper into the electrode. Figure 17 demonstrates this prediction.

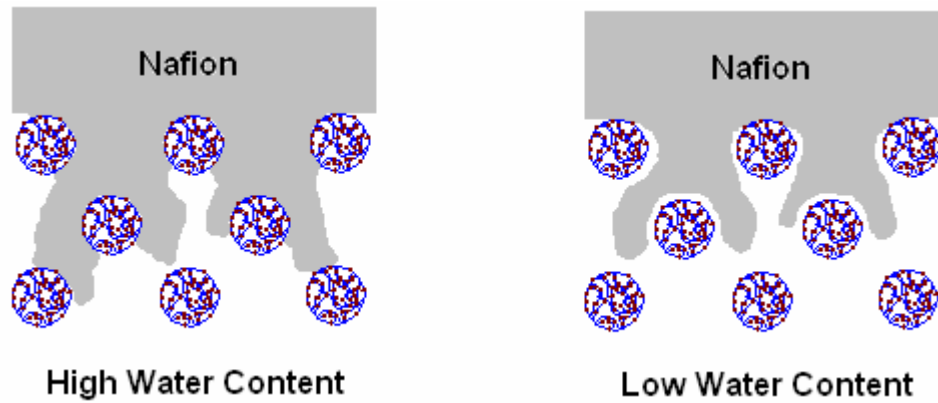


Figure 17 Nafion contacting carbon particles in electrode at high water content (Left) and low water content (Right)

Due to the conditions at which the MEA is fabricated, the Nafion has already deformed a significant depth into the electrode before it is employed in fuel cell. It is uncertain to what extent the Nafion swells inside the electrode due to water content, but it would likely expand to limits of the space it already occupies. The right of Figure 17 shows Nafion after it has contracted due to water evaporation. As the water content increases, the Nafion will swell and contact more of the catalyst on the carbon particles (left of Figure 17). On the small scales with which we are working, expansion in a lateral direction is more significant than expansion deeper into the electrode. The Nafion would have to press much further down to contact the same amount of catalyst reached by a smaller, lateral expansion.

7.2 Importance for MEAs

As exhibited by the SEM images, the temperature at which Nafion is pressed has a very significant effect on the manner in which it deforms. Unless the Nafion is close to its T_g or at a temperature above it, the Nafion will not extrude into small features. This has

important applications in the fabrication of membrane electrode assemblies (MEAs) for PEMFCs. The temperature at which the MEA is fabricated must be well above the T_g of the Nafion in order for the polymer to extrude into the porous electrode surface and contact as much of the catalyst as possible.

If the deformation of the Nafion depends significantly on temperature, then similar behavior is expected by other ionomers. Polystyrene sulfonate (PSS), sulfonated polybenzimidazole (PBI), and sulfonated polyether ether ketone (PEEK) are all ionomers used in PEMFCs that are phase separated with hydrophobic and acidic hydrophilic regions like Nafion. Thus, the MEA procedure should be modified for each different polymer because each has a different glass transition temperature. The smallest size trench into which these polymers will deform is unknown. Investigations such as this thesis would have to be performed for each polymer to determine its behavior, limitations, and ideal pressing conditions.

7.3 Importance for Electrode Morphology

Under no conditions examined in this thesis was Nafion able to completely deform into a 2 μm wide trench. Thus, 2 μm seems to approach the lower limit of sizes into which Nafion can deform. The electrode into which the Nafion is pressed has pore sizes that range from about 100 nm all the way up to 30 μm [20]. As determined by this thesis, the ideal morphology for an electrode is one with pores at least greater than 2 μm and ideally greater than 5 μm . Furthermore, if the electrode were to crack during either assembly or operation, it would create a feature even greater than its pore size into which the Nafion would easily deform. If too much Nafion deforms into the open space, it would contact a

large area of catalyst but fail to permit the gas phase to simultaneously contact the catalyst and therefore decrease performance.

7.4 Importance for Membrane Thickness

This thesis looked at the width of features into which Nafion would deform rather than the depth. However, the silicon was etched to a depth of at least 5 μm , so it can be concluded that at temperatures of 100°C and higher the Nafion had no trouble pushing 5 μm into features with widths of 5 μm and greater. In an effort to obtain more current from fuel cells, membranes are being made thinner and thinner, down to $\sim 25 \mu\text{m}$. The membrane thickness becomes critical when these very thin membranes are used. If the Nafion easily deforms to a depth of 5 μm at 100°C, then it is predicted that it would deform even further at higher temperatures if given the room. Since an electrode is pressed on each side of the membrane, the maximum depth to which the Nafion should deform is half the thickness of the membrane. For membranes as thin as 25 μm , this depth is 12.5 μm , which is trivial considering the porosity of the electrode can be as great as 30 μm . Thus, the electrode morphology is even more important when using thin membranes, as is the temperature and pressure at which the MEA is fabricated.

7.5 Recommendations for further study

At temperatures below the glass transition temperature it is believed that the method by which Nafion deforms resembles a flow pattern. To test this theory, samples can be prepared at similar temperatures (90°C, 100°C, 110°C, etc.) but pressed at various times. If the flow theory is valid, the Nafion should deform further into the trenches at longer times.

One of the major difficulties faced in this thesis was sample preparation for the SEM. The Nafion rarely snapped and consistently pulled away from the silicon substrate in liquid nitrogen. Perhaps, in future experiments, another piece of silicon could be pressed on top of the Nafion so the sample would then consist of a piece of Nafion sandwiched in between two silicon wafers. This arrangement might prevent the Nafion from pulling away so easily. Furthermore, it would offer two chances to see the Nafion deform into the trenches.

In some of the samples a much thinner Nafion membrane was used because it was more likely to snap in the liquid nitrogen. However, this thinner membrane was not pressed at all the temperatures that were tested. In order to see if the thickness of the membrane influences its deformation, both membranes must be tested at every temperature.

As determined in this thesis, a width of 2 microns appears to be a critical size because Nafion never completely pushed into a feature of that size. To more accurately determine the width into which Nafion will not deform, more widths must be tested around 2 microns. This would require fabrication of a new mask with trenches of widths 1, 2, 3, 4, and 5 microns.

It would be useful to know the exact depth to which Nafion was able to extrude at each temperature. To accomplish this, the trenches must be etched to a greater depth than the prevailing $\sim 5\text{ }\mu\text{m}$. A depth of up to $10\text{ }\mu\text{m}$ can be achieved using reactive ion etching, but other methods (such as using a deep silicon etcher) must be used for depths greater than $10\text{ }\mu\text{m}$.

Last, and perhaps the most important, the effect of water content on the deformation of Nafion should be investigated. It is known that Nafion swells considerably when saturated with water. However, in samples that were pressed after being soaked in

water, the Nafion pulled away from the silicon shortly after removal from the press. This occurred at temperatures through 100°C. It would be very valuable to create a technique to bypass this problem so the effect of water content on the deformation of Nafion can be studied.

References

1. Moxley, J.F., S. Tulyani, and J.B. Benziger, *Steady-state multiplicity in the autohumidification polymer electrolyte membrane fuel cell*. Chemical Engineering Science, 2003. **58**: p. 4705-4708.
2. Srinivasan, S., et al., *Fuel Cells: Reaching the era of clean and efficient power generation in the twenty-first century*. Annual Review of Energy and the Environment, 1999. **24**: p. 281-328.
3. Benziger, J., et al., *The Stirred Tank Reactor Polymer Electrolyte Membrane Fuel Cell*. AIChE Journal, 2004. **50**(8): p. 1889-1900.
4. Perry, R.H. and D.W. Green, eds. *Perry's Chemical Engineers' Handbook*. 7 ed. 1997, McGraw-Hill.
5. Yang, C., et al., *Approaches and technical challenges to high temperature operation of proton exchange membrane fuel cells*. Journal of Power Sources, 2001. **103**: p. 1-9.
6. Hogarth, W.H.J., J.C.D.d. Costa, and G.Q.M. Lu, *Solid acid membranes for high temperature (>140C) proton exchange membrane fuel cells*. Journal of Power Sources, 2005. **142**: p. 223-237.
7. Doyle, M. and G. Rajendran, *Perfluorinated Membranes*. Handbook of Fuel Cells: Fundamentals, Technology, and Applications, ed. W. Vielstich, A. Lamm, and H.A. Gasteiger. Vol. 3. 2004, England: John Wiley & Sons Ltd.
8. Seen, A.J., *Nafion: An Excellent Support for metal-complex catalysts*. Journal of Molecular Catalysis A: Chemical, 2001. **177**: p. 105-112.
9. DuPont, *FluoroIntermediates: Products and Services*. 2005.
10. IUPAC, *Glossary of Basic Terms in Polymer Science*. Pure and Applied Chemistry, 1996. **68**(8): p. 1591-1595.
11. Yeo, S.C. and A. Eisenberg, *Physical Properties and Supramolecular Structure of Perfluorinated Ion-Containing (Nafion) Polymers*. Journal of Applied Polymer Science, 1977. **21**: p. 875-898.
12. Gierke, T.D., G.E. Munn, and F.C. Wilson, *The Morphology in Nafion Perfluorinated Membrane Products, as Determined by Wide- and Small- Angle X-ray Studies*. Journal of Polymer Science: Part B: Polymer Physics, 1981. **19**: p. 1687-1704.
13. Yeager, H.L. and A. Steck, *Cation and Water Diffusion in Nafion Exchange Membranes: Influence of Polymer Structure*. Journal of the Electrochemical Society, 1981. **128**(9): p. 1880-1884.
14. Eisenberg, A. and T. Sasada. in *Second International Conference of the Physics of Non-Crystalline Solids*. 1964.
15. McCrum, N.G., *An Internal Friction Study of Polytetrafluoroethylene*. Journal of Polymer Science, 1959. **34**(127): p. 355-369.
16. DuPont, *Product Information: Nafion PFSA Membranes*. 2002, DuPont: Fayetteville, NC. p. 4.
17. Thampan, T., et al., *PEM fuel cell as a membrane reactor*. Catalysis Today, 2001. **67**: p. 15-32.
18. Adamson, A.W. and A.P. Gast, *Physical Chemistry of Surfaces*. 6 ed. 1997, New York: John Wiley & Sons, Inc.

19. Rosen, S.L., *Fundamental Principles of Polymeric Materials*. 2 ed. 1993, New York: John Wiley & Sons, Inc.
20. Mathias, M.F., et al., *Diffusion media materials and characterisation*. Handbook of Fuel Cells: Fundamentals, Technology, and Applications, ed. W. Vielstich, A. Lamm, and H.A. Gasteiger. Vol. 3. 2004, England: John Wiley & Sons Ltd.

Appendices

Photolithography Recipe

1. Solvent clean silicon wafers with Acetone first, then Isopropanol, then dry with N₂.
2. Dehydrate bake on hot plate at 110°C for at least 15 minutes.
3. Spin on HMDS⁶ using spinner recipe 1 (40 seconds at 4,000 rpm)
4. Spin on AZ5214 photoresist using spinner recipe 1 (40 seconds 4,000 rpm)
5. Soft bake on hot plate at 95°C for 1 minute.
6. Use Karl Suss MA6 Mask Aligner with following parameters for exposure:
 - Exposure time: 25 seconds
 - Contact: Hard Contact
 - CL1 = 2.0mW/cm²
 - Alignment gap: 60μm
 - WEC = contact
7. Develop resist for 25-30 seconds in a mixture of 1:1 AZ MIF312: DI H₂O
8. Thoroughly rinse wafer (30+ sec) in DI H₂O, dry with nitrogen.
9. Inspect under optical microscope with green filter (to avoid exposing the photoresist again)
10. Hard bake at 110°C for 6 minutes.

⁶ Note: HMDS improves the adherence of the photoresist to the silicon wafer

Additional SEM Pictures at 90°C

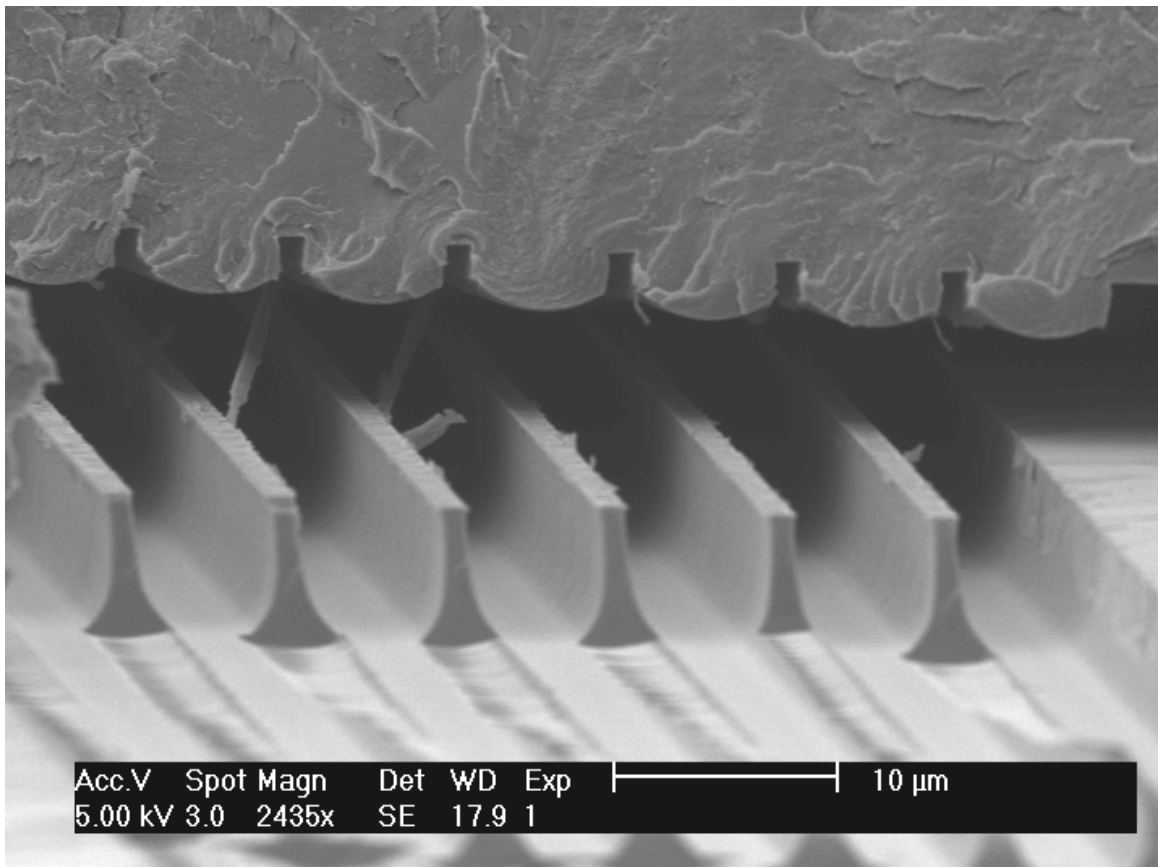


Image 9 SEM Image of 5 micron trench separated by 2 microns pressed at 90C (sample 27).

Nafion is on the top, silicon is on the bottom. Even though the Nafion is slightly separated from the silicon, it is evident that the 5 micron features did not press all the way to the bottom of the trench. Nafion's radius of curvature is the same as the trench.

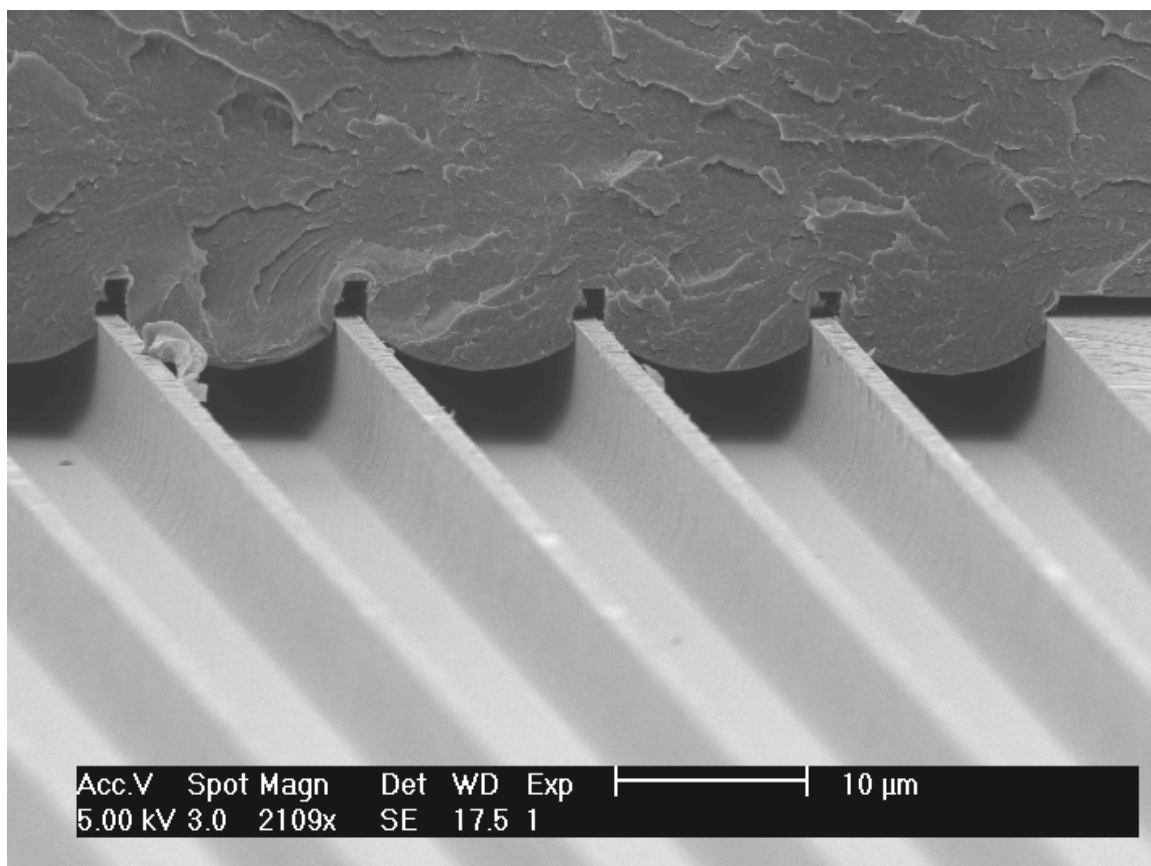


Image 10 SEM Image of 10 micron wide trench separated by 2 microns pressed at 90C (sample 27).

Nafion is on top, silicon is on the bottom. Even at a width of 10 microns the Nafion did not take on the shape of the bottom of the trench.

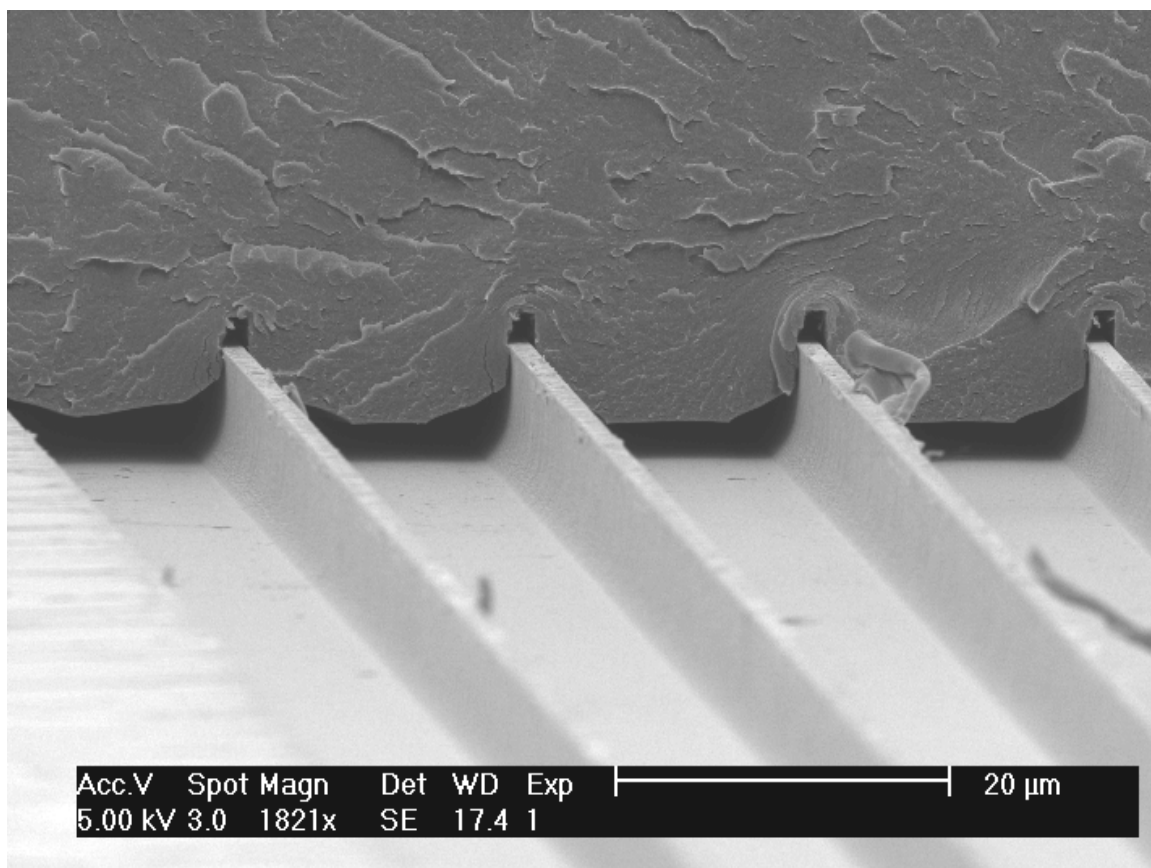


Image 11 SEM Image of a 15 micron wide trench separated by 2 microns pressed at 90C (sample 27)

Nafion is on the top, silicon is on the bottom. At a width of 15 microns the Nafion reached the bottom (as evident from the flat part) but did not deform completely into the trench (as evident from the angled corners).

Additional SEM Images at 100°C

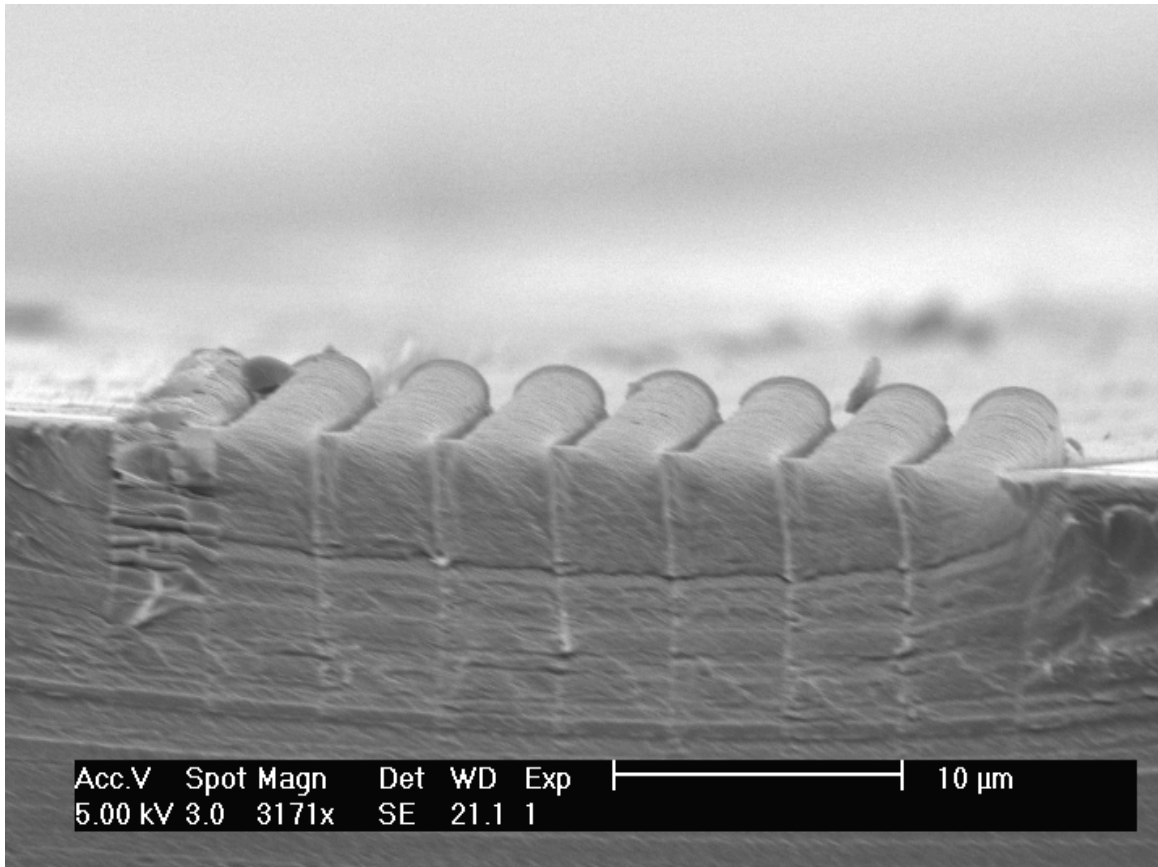
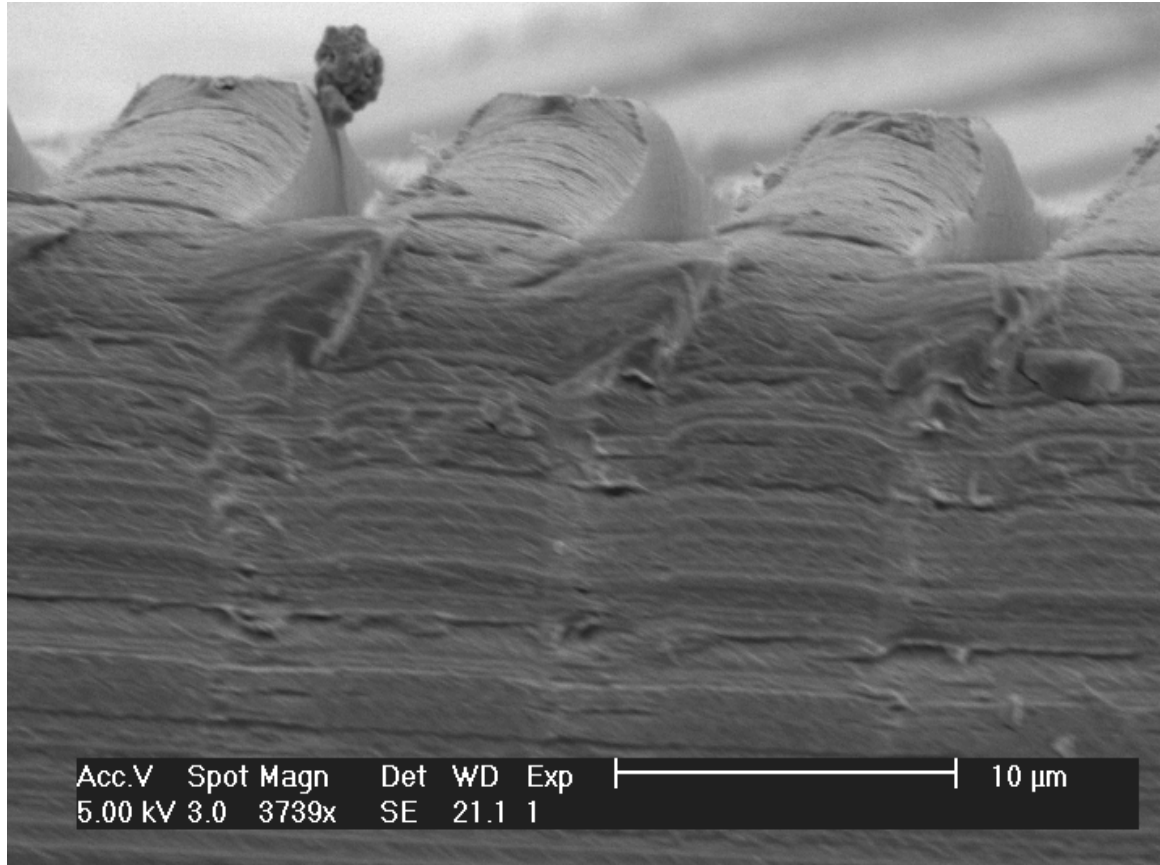


Image 12 SEM Image of 2 micron wide features separated by 2 microns at 100C (sample 17)

Only Nafion is shown here because it separated from the silicon wafer. From the shape of the top of the feature you can tell it did not reach the bottom of the trench because it did not take on the shape of the trench. Notice that the curvature is the same as the trench.



**Image 13 SEM Image of 5 micron features raised in Nafion
separated by 5 microns pressed at 100C (sample 17)**

Only Nafion is shown here because it separated from the silicon wafer. From the shape of the top of the feature you can tell it deformed all the way into the trench because it assumed the shape of the trench. Striations are visible in the Nafion as a result of it still being in its glassy state.

Additional SEM Pictures at 110°C

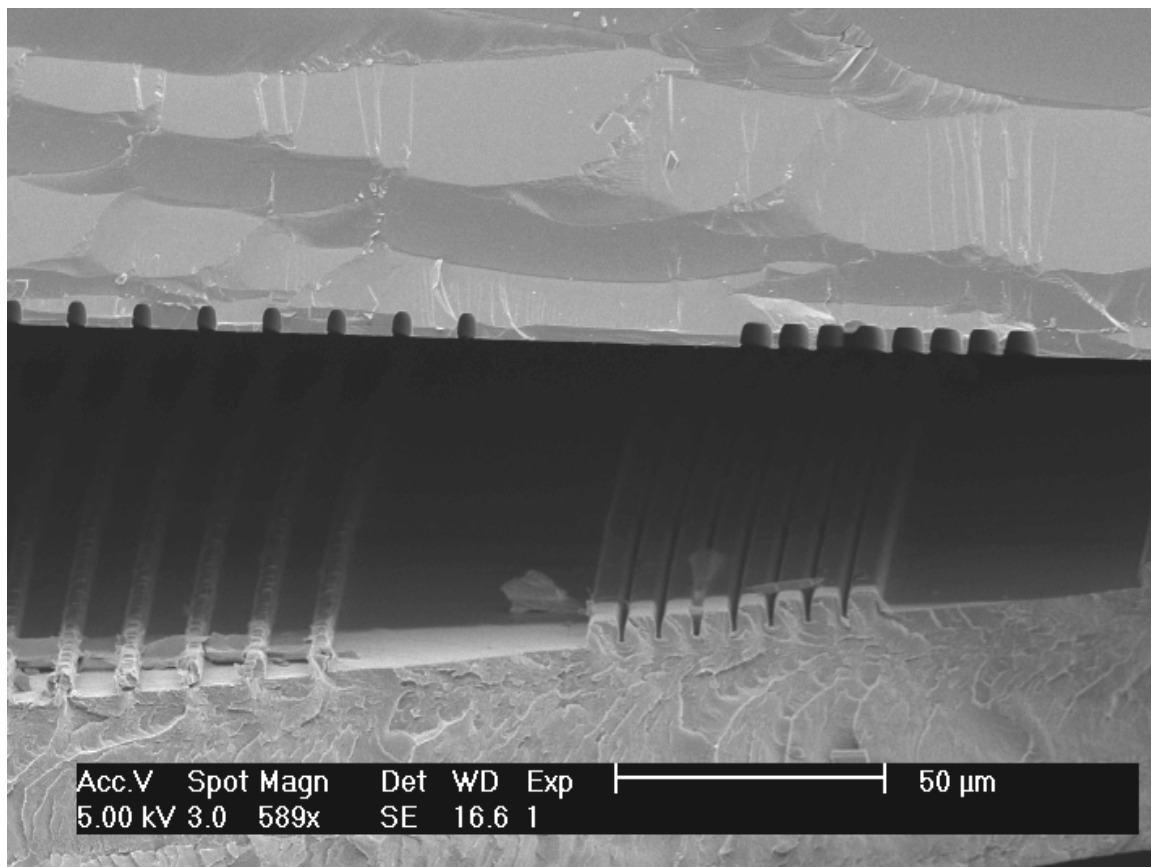


Image 14 SEM Image of silicon (top) pulled away from Nafion (bottom) pressed at 110C (sample 34)

The trenches to the right in Image 14 are 5 microns wide and separated by 2 microns. You can tell from the flat tops that the Nafion reached the bottom of the trench, whereas it did not for the 2 micron wide features on the left.

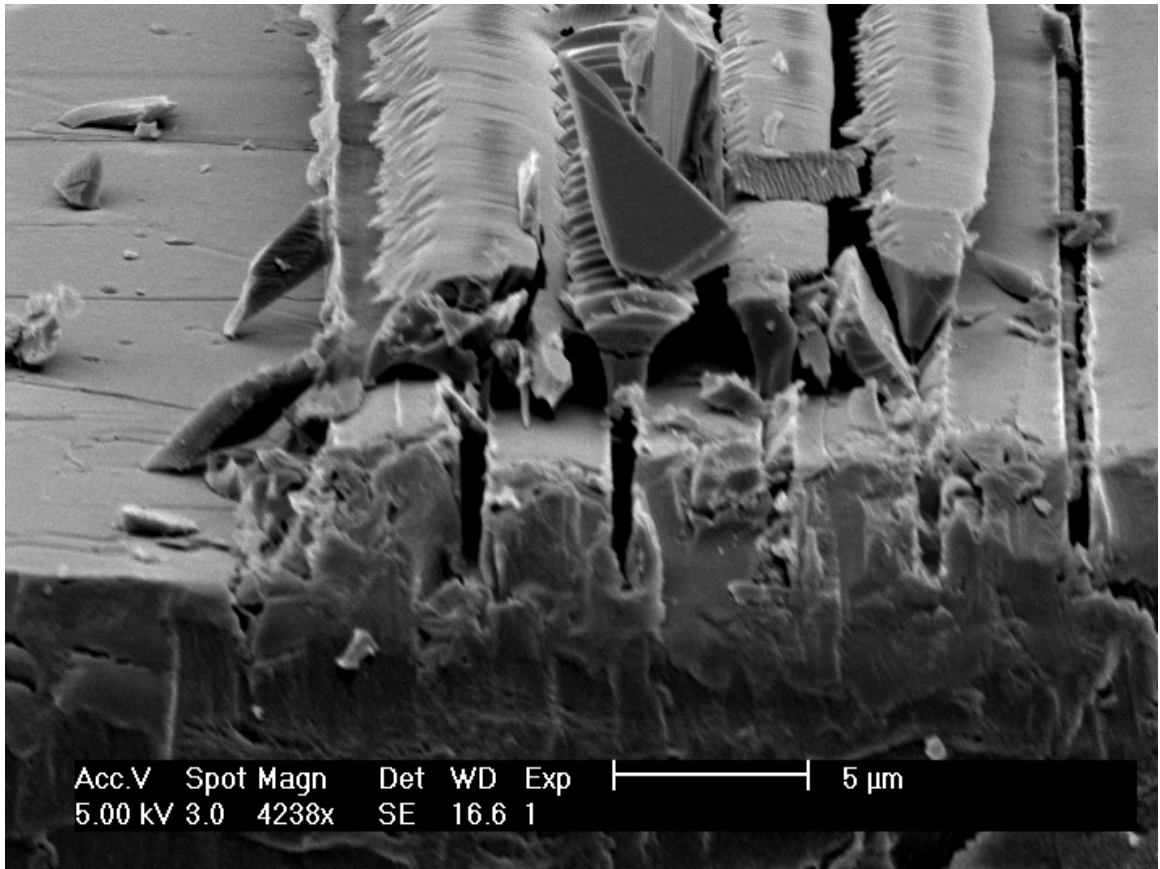


Image 15 SEM Image of 2 micron features separated by 2 microns pressed at 110C (sample 34)

The Nafion is on the bottom and pieces of the silicon wafer remain embedded on top.

Obviously the 2 micron features did not reach the bottom of the trench and they also don't show a reverse curvature.

Additional SEM Pictures at 140°C

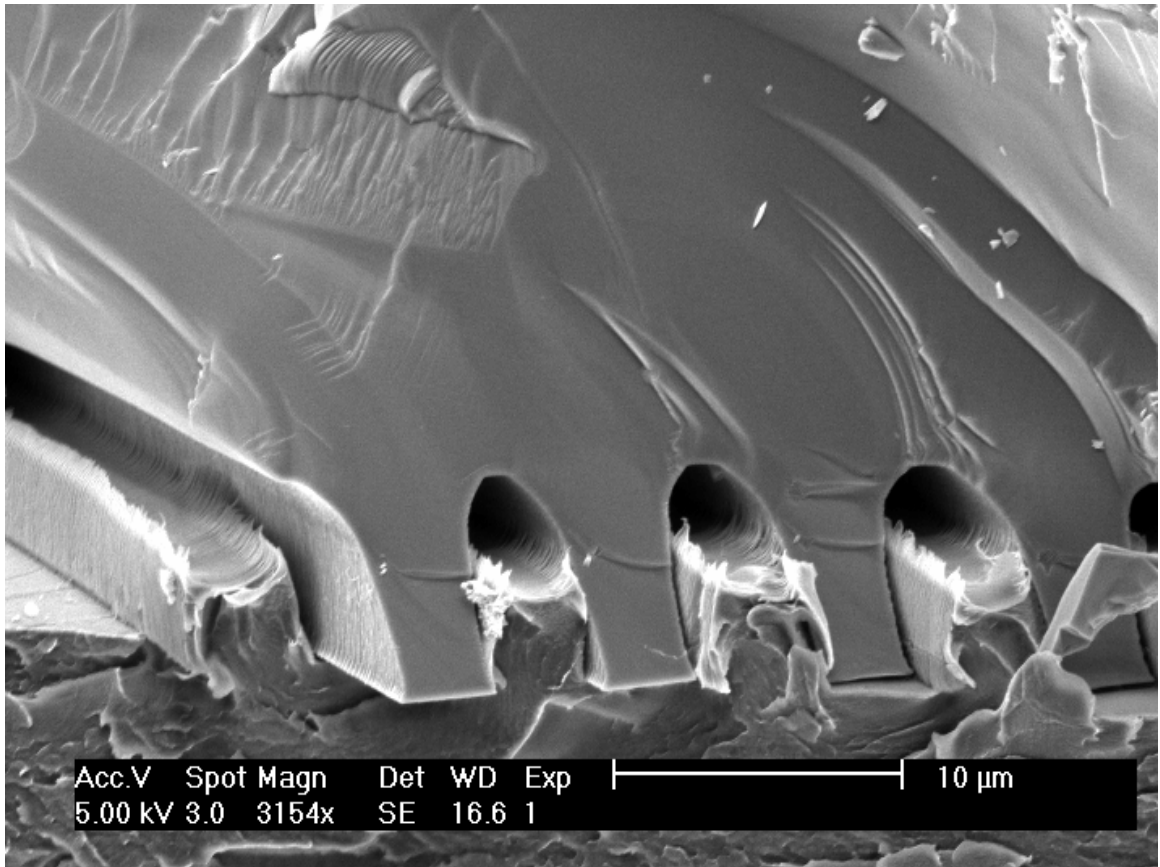


Image 16 SEM image of 2 micron wide trenches separated by 5 microns pressed at 140C (sample 4)

The Nafion is on the bottom and the silicon is on the top. All the two micron features exhibit the reverse curvature that corresponds to wetting.

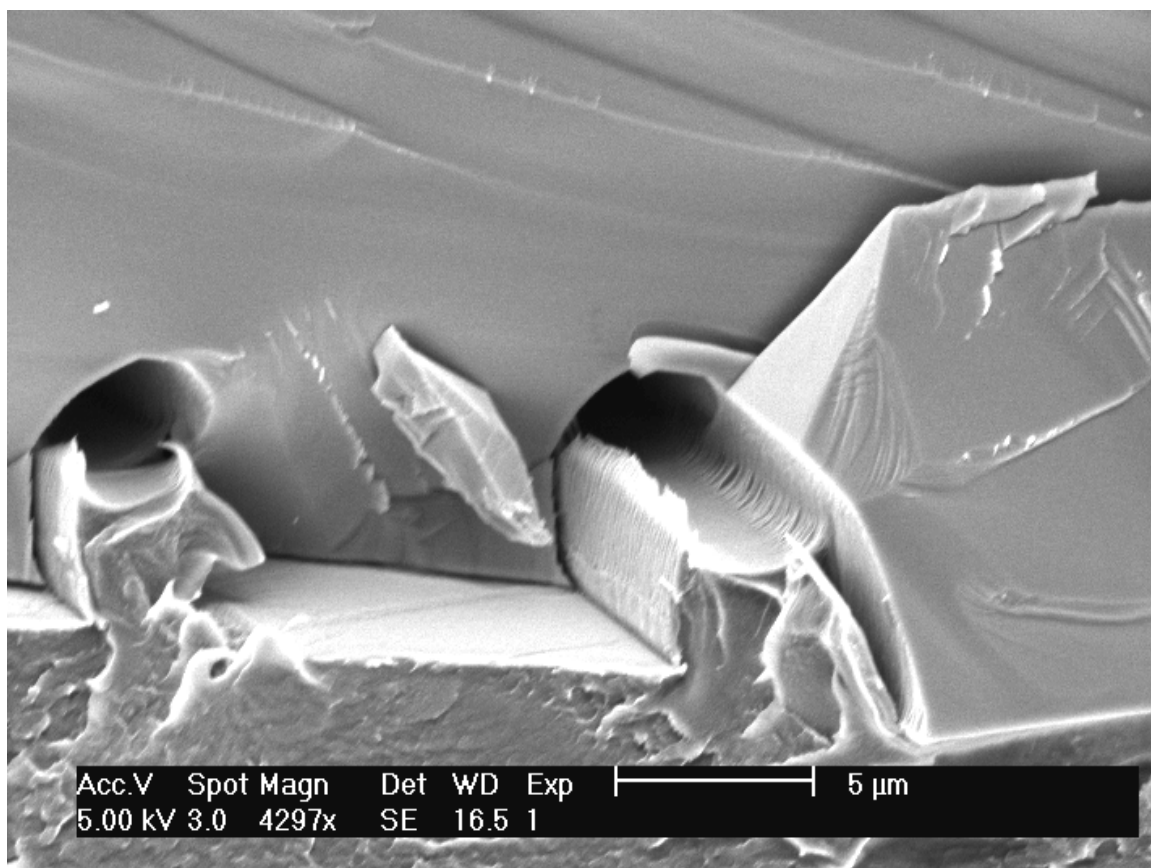


Image 17 SEM image of 2 micron wide trenches separated by 10 microns pressed at 140C (sample 4)

The Nafion is on the bottom and the silicon is on the top. All the two micron features exhibit the reverse curvature that corresponds to wetting.

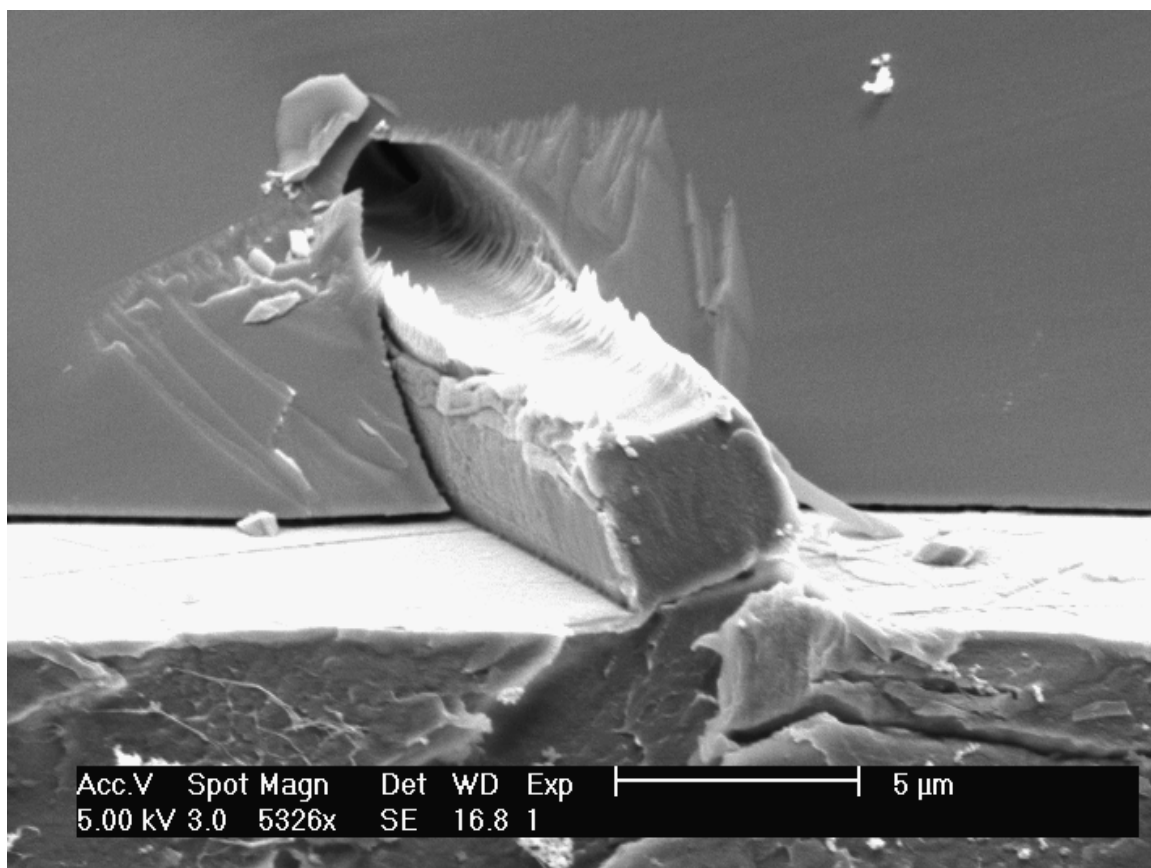


Image 18 SEM image of 2 micron wide trench pressed at 140C (sample 4)

The Nafion is on the bottom and the silicon is on the top. All the two micron features exhibit the reverse curvature that corresponds to wetting.

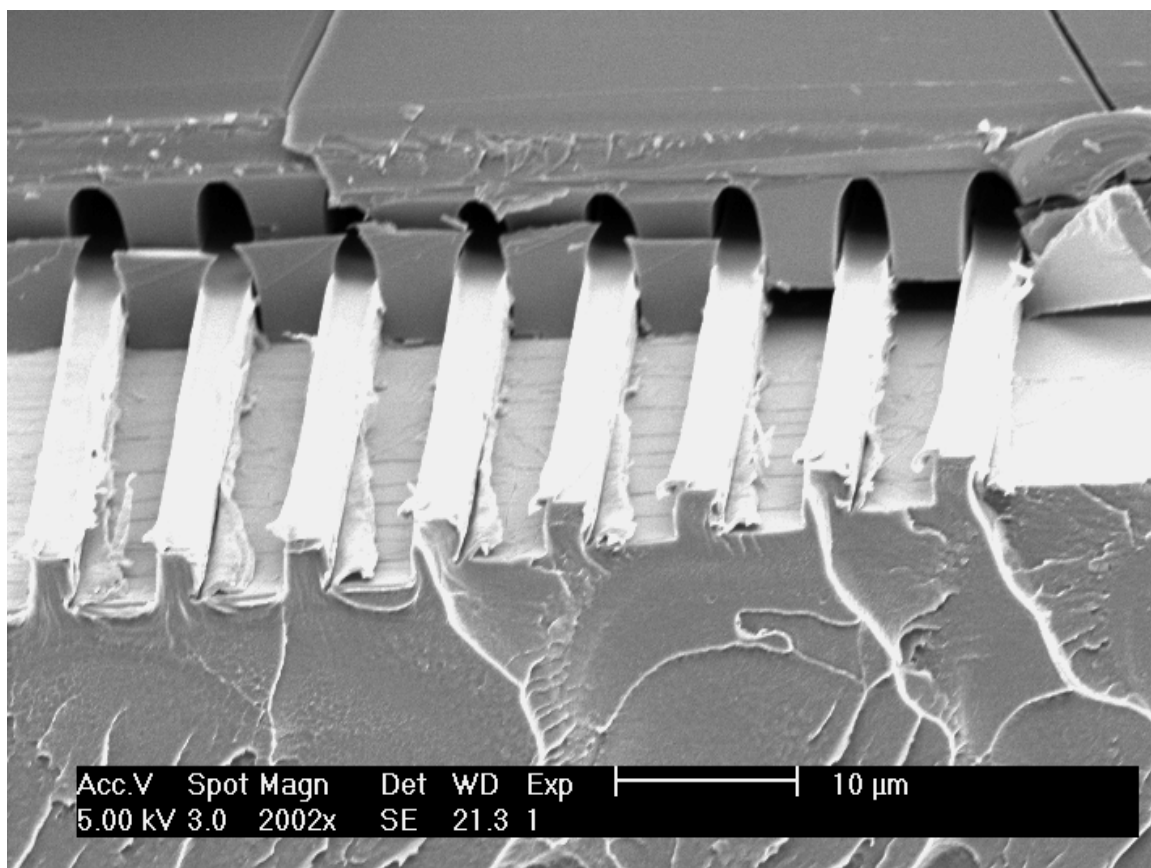


Image 19 SEM image of 2 micron wide trenches pressed at 140C (sample 15)

The Nafion is on the bottom and the silicon is on the top. All the two micron features exhibit the reverse curvature that corresponds to wetting.

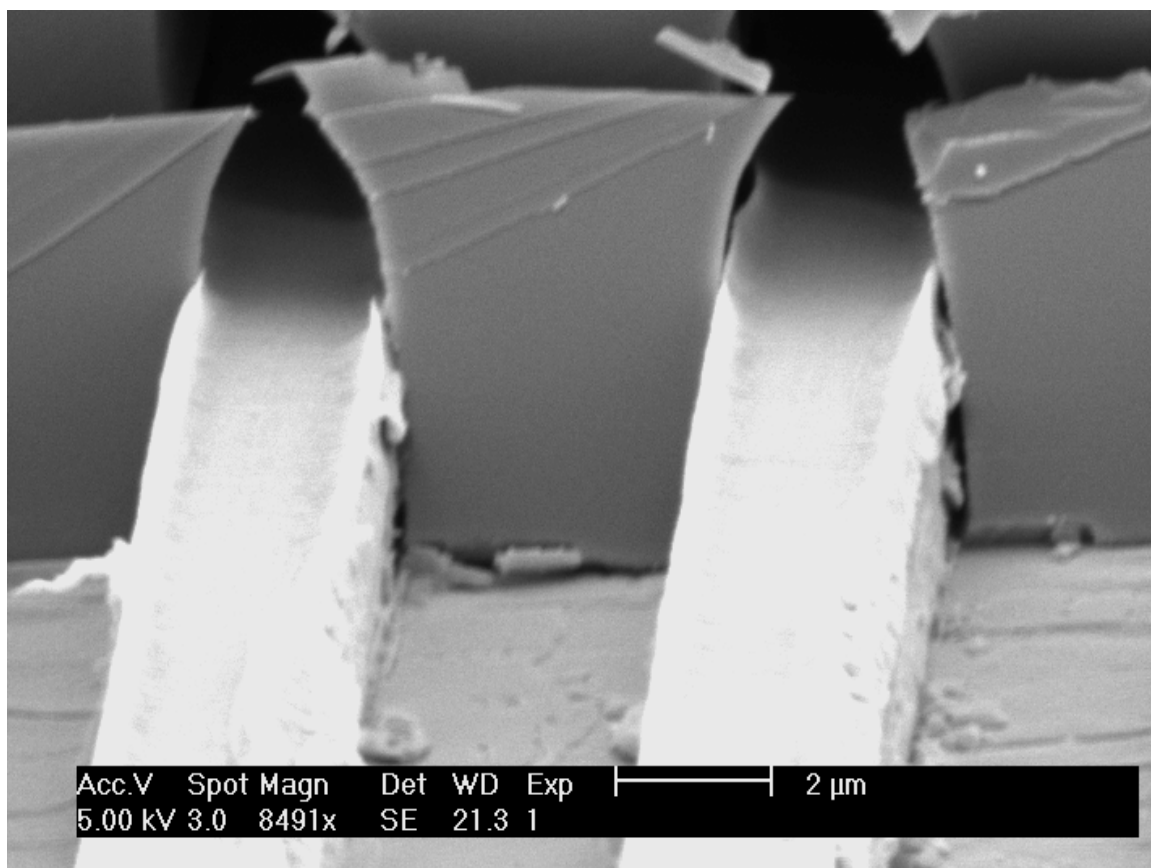


Image 20 SEM image of 2 micron wide trenches pressed at 140C (sample 15)

The Nafion is on the bottom and the silicon is on the top. All the two micron features exhibit the reverse curvature that corresponds to wetting.

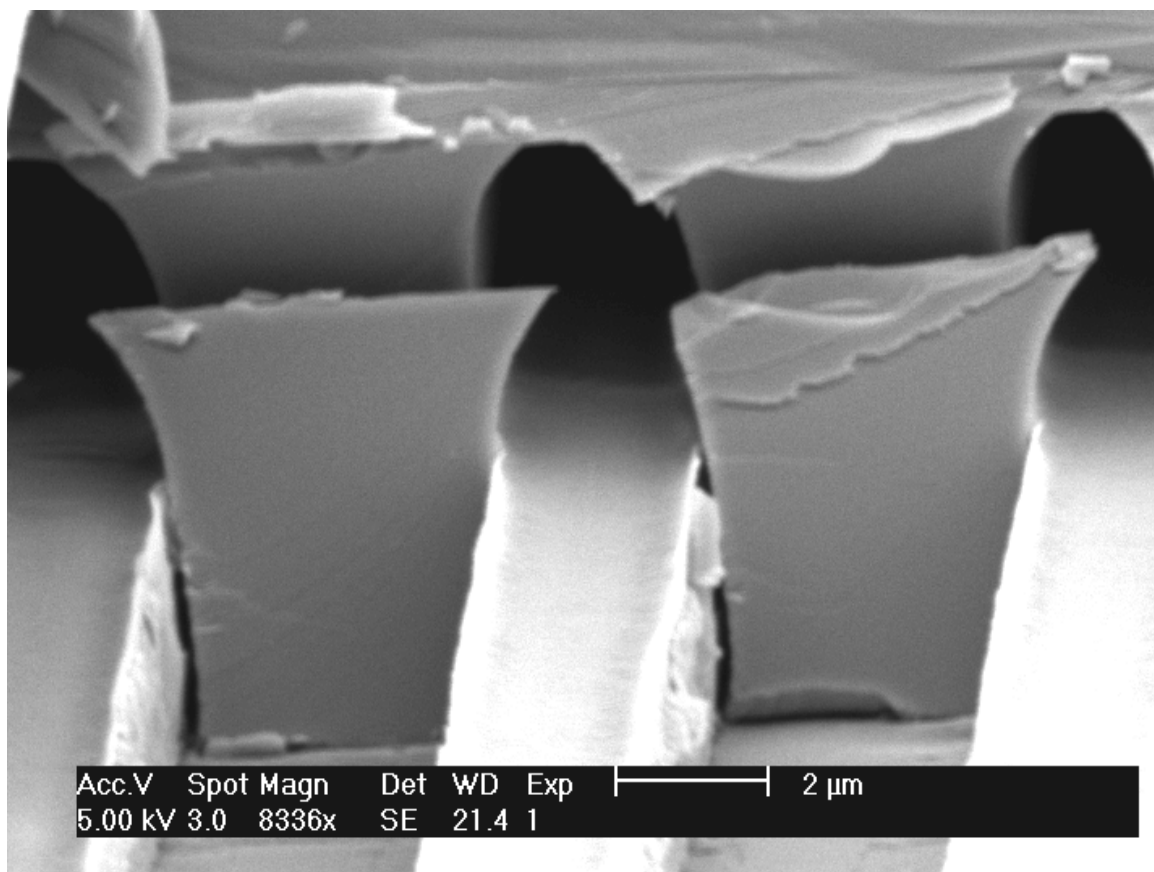


Image 21 SEM image of 2 micron wide trenches pressed at 140C (sample 15)

The Nafion is on the bottom and the silicon is on the top. All the two micron features exhibit the reverse curvature that corresponds to wetting.

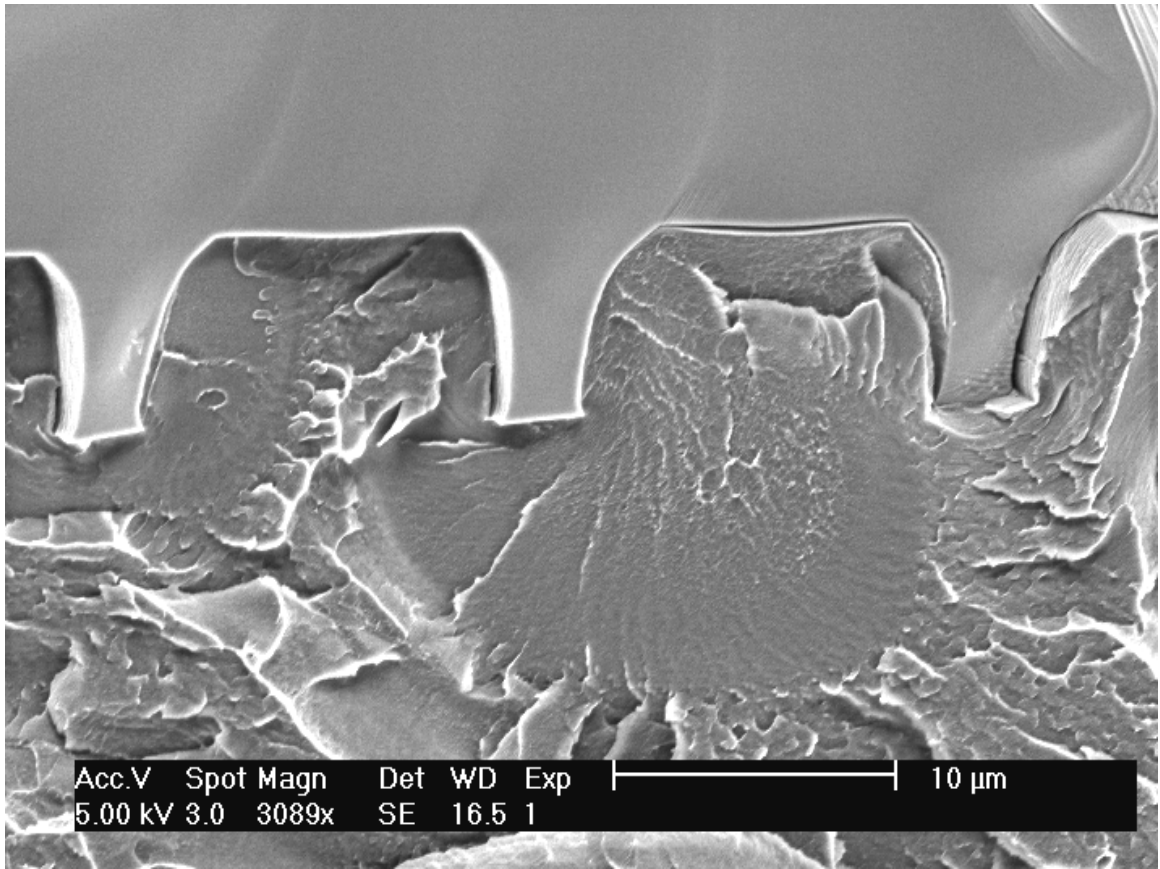


Image 22 SEM image of 10 micron wide trenches separated by 5 microns pressed at 140C (sample 4)

The Nafion is on the bottom and the silicon is on the top. The Nafion completely deformed into all features with widths of 5 microns or greater.